Synthesis and gelation assessment of functionalized diphenylalanine dipeptides - towards cell culture applications

M.Sc. thesis

University of Jyväskylä

Department of Chemistry

20.12.2023

Noora Heiskanen

ABSTRACT

The literature part of this master's thesis discusses the usage of hydrogels in cell culture. It goes through the microenvironmental aspects that need to be considered when choosing a hydrogel for cell culture. The differences between natural, synthetic and hybrid hydrogels are explained, and examples of hydrogels used in biomedical applications are described.

The aim of the experimental part was to synthesise 9-fluorenylmethyloxycarbonyl-protected diphenylalanine dipeptide (FmocFFCOOH) and cinnamoyl-protected diphenylalanine dipeptide (CinFFCOOH) to compare their gelation properties. The nuclear magnetic resonance (NMR) spectroscopic, high-resolution mass spectrometric (HR-MS) and Fourier-transform infrared (FT-IR) spectroscopic analyses were performed to identify the products and prove their purities. For FmocFFCOOH, the conducted gelation trials showed promising results. Unfortunately, for CinFFCOOH, there was not enough clean product or time to do gelation analysis.

TIIVISTELMÄ

Tämän tutkielman kirjallisuuskatsaus käsittelee soluviljelyssä käytettyjä hydrogeelejä. Tutkielmassa käydään läpi soluviljelyn asettamia vaatimuksia hydrogeeleille sekä esitetään jo tunnettuja hydrogeelejä, niiden eri luokkia, ominaisuuksia ja eroja. Lopuksi tutustutaan hydrogeelien erilaisiin sovellusmahdollisuuksiin biolääketieteessä.

Kokeellisen osan tavoitteena oli syntetisoida kaksi suojattua dipeptidiä ja vertailla niiden geeliytymisominaisuuksia. Syntetisoidut dipeptidit olivat 9-fluorenyylimetyylioksikarbonyyli-suojattu difenyylialaniinidipeptidi (FmocFFCOOH) ja kinnamoyyli- suojattu difenyylialaniinidipeptidi (CinFFCOOH). Synteesituotteiden tunnistamiseen ja puhtauden määrittämiseen käytettiin ydinmagneettista resonanssispektroskopiaa (NMR), infrapunaspektroskopiaa (FTIR) ja korkean resoluution massaspektrometriä. FmocFFCOOH:lle tehdyissä gelaatiokokeissa saatiin lupaavia tuloksia. Valitettavasti CinFFCOOH:lle ei saatu tehtyä haluttuja gelaatiokokeita ja analyysejä, sillä puhdasta reaktiotuotetta ei ollut käytettävissä riittävästi.

PREFACE

This master's thesis was made at the Nanoscience Center of the University of Jyväskylä. The experimental part was started in the autumn of 2022 and finished in January 2023. The literature part was started in August 2023 and completed during autumn 2023. The supervisors for my thesis were Professor Maija Nissinen and Postdoctoral Researcher Efstratios Sitsanidis. I would like to thank both for the advice and guidance during the process. I would also like to thank Arto Valkonen for being the external examiner of the thesis.

TABLE OF CONTENTS

ABBREVIATIONS

Ala	alanine
APA	ammonium persulfate
Azo	azobenzene
Boc	*N*-*tert*-butoxycarbonyl
Cbz	carboxybenzyl
Cin	cinnamoyl group
d	doublet (NMR)
dd	doublet of doublets (NMR)
DCM	dichloromethane
DMF	dimethylformamide
DMSO	dimethyl sulfoxide
DNA	deoxyribonucleic acid
EA	ethyl acetate
ECM	extracellular matrix
Eq	equivalent
Fmoc	9-fluorenylmethoxycarbonyl group
FTIR	fourier transform infrared spectroscopy
Gly	glycine
HA	hyaluronic acid
Hex	hexane
in vivo	test made in living organism
in vitro	test made in test tube
in situ	tests with living organisms but outside their natural environment
LMWG	low molecular weight gel
Leu	leusine
m	multiplet (FTIR/NMR)
MIP	mercury intrusion porosimetry
Nap	naphthalene
PAM	polyacrylamide

PBS	phosphate-buffered saline
PEG	polyethylene glycol
PEGDA	polyethylene glycol diacrylate
Phe (F)	phenylalanine
PLA	polylactic acid
PPy	polypyrrole
PTZ	phenothiazine
PVA	polyvinyl alcohol
PVP	polyvinylpyrrolidone
Pyr	pyrene
RNA	ribonucleic acid
RGD	arginylglycylaspartic acid
s	sharp (FTIR), singlet (NMR)
SEM	scanning electron microscopy
sh	shoulder (FTIR)
TBTU	2- (1H-benzotriazole-1-yl)-1,1,3,3-tetramethyl ammonium tetrafluoroborate
*t*Bu	*tert*-butyl group
TEMED	tetramethylethylenediamine
vw	very wide (FTIR)
w	wide (FTIR)

LITERATURE PART

1 Introduction

Low molecular weight gels (LMWGs) constitute a group of soft viscoelastic materials that form when small molecules self-assemble to a network able to immobilize solvent. Gels are present in everyday products, for example, diapers, contact lenses and wound dressings. Existing gels can be classified based on the solvent and gelation trigger into different types, namely hydrogels, organogels, xerogels, physical and polymeric gels, etc. [1]

Hydrogels are a significant category of gels constructed when a hydrogelator self-assembles in water (or in other aquatic solutions, e.g., a buffer solution). The gelation of a compound is not straightforward, and it varies hugely, depending on the conditions, such as solution, temperature and pH. The basic gelation process is solubilizing or dispersing the compound and then triggering the start of the gelation. Common triggers are, for example, heating and cooling, pH change, solvent exchange, and sonication. The gelation method and gelation process affect the gel properties. So, the same molecule can have different properties in its gel form depending on the gelation process. Even with the simplest method, heating and cooling, there are still many process variables, such as, the heating/cooling time and temperature. Changing these variables can result in different outcomes.[1]

Another commonly used method for gelation is solvent exchange. In solvent exchange the compound is dissolved in an organic solvent, like DMSO. Then the solution is mixed with a different solvent, for example water, to trigger the gel formation. Here, the key parameters are the ratio of the solvents and their type. The third important method to trigger gelation is pH change, where the triggering happens by changing the pH of the solution. A low rate of repeatability is usually the main challenge with this method. Also, an extreme (high or low) pH may break the molecular structure.[1]

The experimental part shows the synthetic process behind forming a hydrogel that could be used in cell culture. The experimental part focuses on the two syntheses of cinnamoyl-protected diphenylalanine dipeptide (CinFFCOOH), which we compare to a known hydrogelator fluorenylmethyloxycarbonyl-protected diphenylalanine dipeptide (FmocFFCOOH). The gelation ability of diphenyl dipeptide containing a cinnamoyl group is studied, as it has been previously observed that the cinnamoyl moiety is the smallest structural motif in functionalized phenylalanine to be considered an effective hydrogelator. The synthesis of CinFFCOOH was done according to a previously published protocol[2].

These types of LMW hydrogels could bring applications to food processing, cosmetics, drug delivery, and other biomedical applications, due to their properties.[3,4] The objectives of this study were to learn new synthesis techniques such as dry reaction conditions, amide bond formation and selective protection and deprotection protocols. Also familiarising with gelation triggers and their techniques was experimented.

2 Classification and usage of different types of hydrogels

Hydrogels can be classified by multiple factors, such as the origin of the source, composition, structure configuration, cross-linking, network charge, durability, and their response to external stimuli.[5] Here, the classification is based on their origin. This classification is divided into natural, synthetic and hybrid hydrogels, depending on their constituent properties.[6] Figure 1. shows the advantages and disadvantages of these three hydrogel classes.

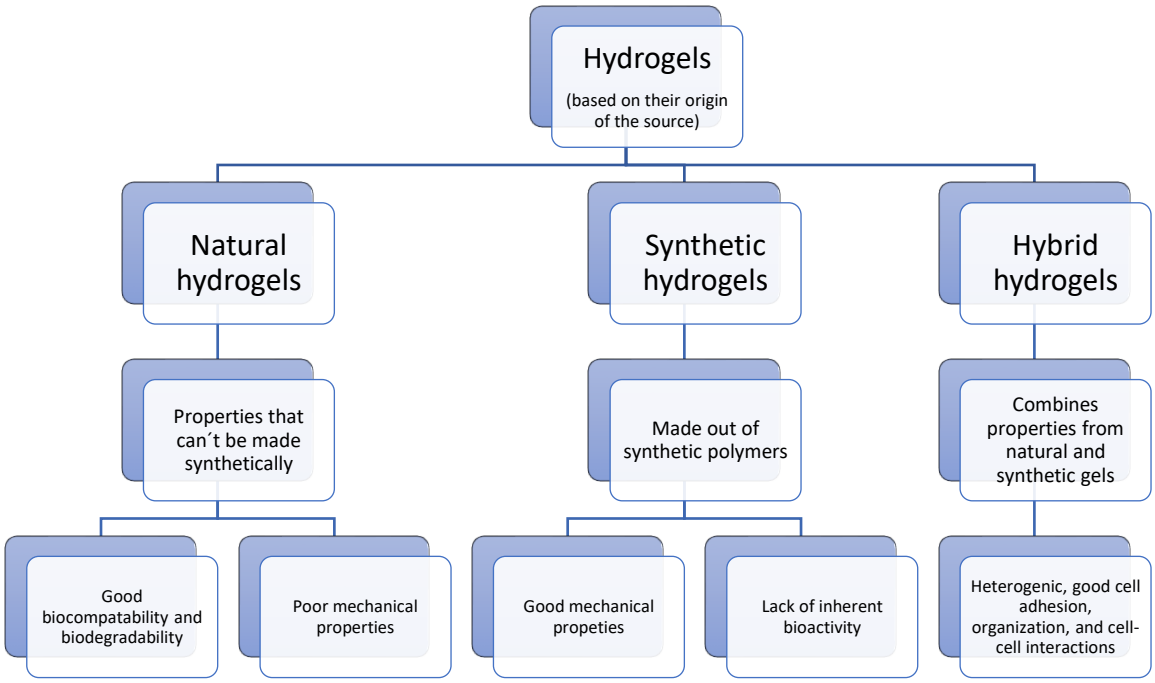

Figure 1. Classification of hydrogels based on their source.

2.1 Natural hydrogels

Natural hydrogels have strong cell adhesion capabilities, which makes them biocompatible and, biodegradable, and they contain biologically recognizable moieties. Natural hydrogels are usually derived from proteins (collagen, gelatin) or polysaccharides (chitosan). However, natural hydrogels tend not to have good mechanical properties. Also, they might trigger immune/inflammatory responses upon introduction to the human body.[7]

Hydrogel formulation can be done via liquid precursor solutions to make a solid gel-like material. Solidification can be performed by cross-linking, either physically (non-covalent) or chemically (covalent). In the majority of peptide and protein-based systems (e.g., collagen hydrogels), self-assembling occurs via physical cross-linking.[8] Cross-linking of polymer chains affects their physical properties, for example, elasticity, viscosity, solubility, strength, toughness, and melting point. It also increases the molecular weight of the polymer chains, degreasing their solubility.[7]

Physical cross-linking is based on self-assembly generated by intermolecular interactions by hydrophobic groups, hydrogen bonding or electrostatic attraction. The advantages of physically cross-linked hydrogels are their easy synthesis and lack of separate crosslinkers. Physical cross-linking methods and interactions include ionic interactions, hydrogen bonding, maturation (heat-induced aggregation), and hydrophobic interactions.[5]

Chemical cross-linking is based on cross-linking via the formation of covalent chemical bonds. Polymers (natural and synthetic) can be cross-linked via their functional groups, such as amino, carbonyl and hydroxyl groups. Chemical cross-linking can, therefore, be performed by methods like Schiff base reactions (reactions between amino. and aldehyde groups), photo cross-linking and free radical polymerization, and chemical reactions of complementary groups. [5,7]

2.1.1 Collagen

Collagen, constructed of amino acid sequences, is naturally found in the human body mostly in the form of fibrils. There are at least 28 types of collagens; the defining characteristics of collagen are quite loose.[9] Over 90% of the collagen found in the human body can be divided into types I, II and III, where the most common one is type I collagen. The collagen used in hydrogels is commonly type I usually isolated from animal tissue (e.g., bovine, porcine, rat specimens, marine) but also recombinant sources. The isolation is done using acid or enzymes such as pepsin.[8,9]

Type I collagen is a triple helical protein whose fibrils self-assemble into bundled fibers at neutral pH and produce a matrix structure.[10] Free functional groups of collagens (amines and carboxyl) can be used to create physical or chemical cross-links to modify the structure. Due to this ability, collagen can form intra- and interfibrillar cross-links that help create various mechanical properties. [9]

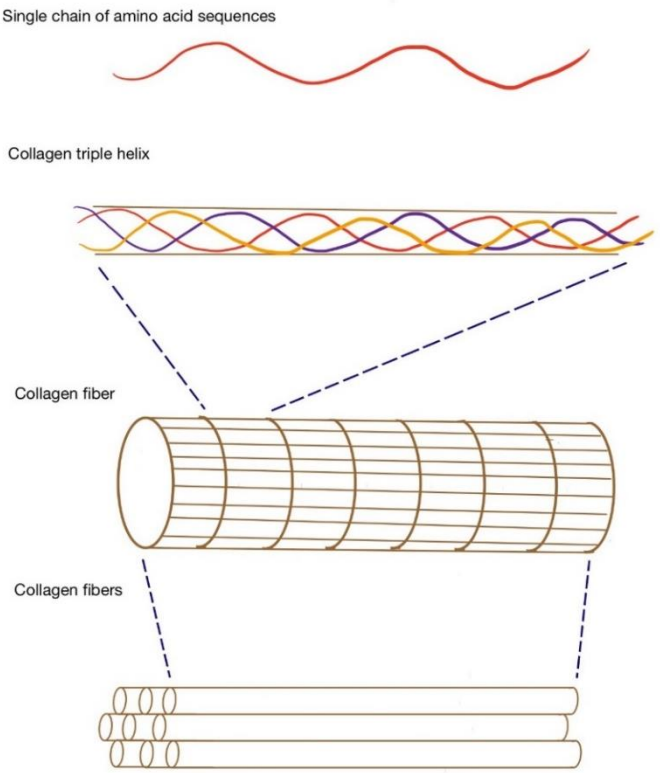

Figure 2. Structure of collagen starting from single acid sequences to form collagen triple helix, continuing to form collagen fiber and later collagen fibers.

The benefits of using collagen are its properties like biocompatibility, biodegradability, porosity, and collagen-to-cell ligand binding. It also has benefits in cell culture because of its ability to establish chemical and biological gradients. Its microstructure has a direct influence on tissue-specific mechanical parameters, and cellular migration. It is a good choice when studying cell encapsulation and cell migration. Collagen hydrogels are best studied when searching platforms for drug delivery and *in situ* tissue engineering.[9] It has also been used in studies to construct *in vivo* tumour microenvironments, *in vitro* neural works, and *in vitro* microvascular networks.[11]

2.1.2 Fibrin

Fibrin is also a natural polymer found in the human body. It forms to a wound during blood coagulation. Fibrin (Figure 3) is formed by thrombin-initiated aggregation of insoluble polypeptide chains of fibrinogen into a network of fibrils.[12] The self-assembling occurs by hydrogen bonds. In the network, additional cross-linking happens via factor XIIIa to produce fibrin mesh. When making fibrin hydrogel, fibrin is at first isolated from blood plasma. Then, it is converted to a fibrin monomer with thrombin and $CaCl_3$, after which the monomers self-assemble by hydrogen bonds and form insoluble fibrin.[11,13]

The advantage of using fibrin for 2D and 3D cell cultures is that it contains naturally cell-binding sites, extracellular matrix (ECM) proteins and growth factors, making it modifiable. Fibrin also presents unique viscoelastic properties that can´t be found in synthetic hydrogels. However, the existing natural cell binding sites make it also usable for hydrogel fabrication without modifications. Previously, its non-linear elasticity was considered a disadvantage, so stiffing the hydrogel for 3D cell culture was intended. It has been noted that softness gives more advantages than disadvantages, for example, in neuro cell studies, as they are naturally very soft tissue.[12,13]

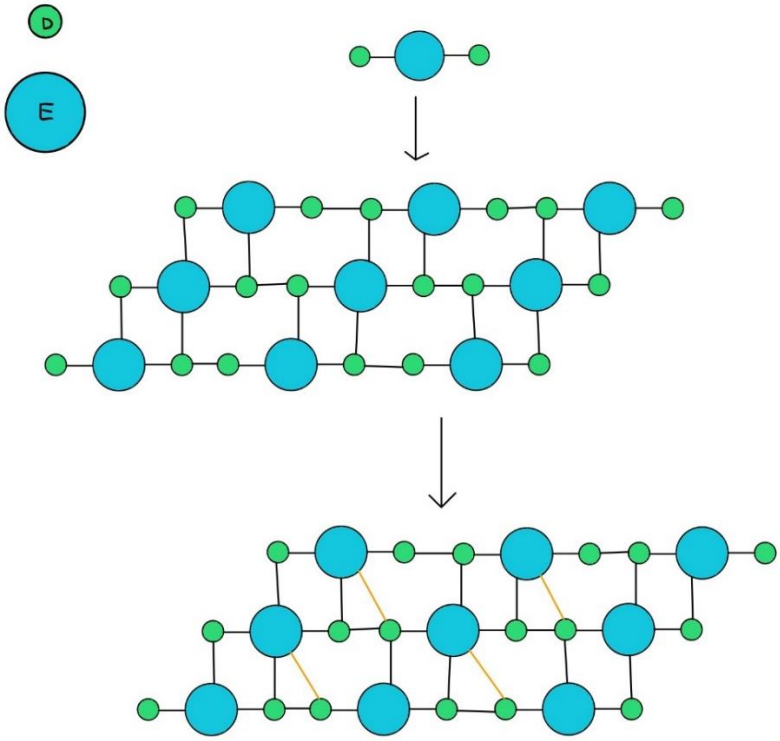

Figure 3. Fibrinogen formation from D-domain and E-domain to make cross-linked fibrin mesh.

Problems with using fibrin also come with its mechanical properties. Luckily, modifications can be done to adjust these issues, such as matching to human spinal cord tissues. Another issue is the rapid degradation rate, which makes it unsuitable for bone and cartilage tissue engineering alone. Fortunately, it can be combined with stable and hard materials to broaden its usage.[13]

2.1.3 Alginate

Alginate is a polysaccharide derived from brown algae and produced by two types of bacteria, *Azotobacter* and *Pseudomonas*. Alginate extraction involves dehydration of algae with the help of alkali solutions like brine. Alginates that are extracted from different sources differ in their existing copolymers. The blocks that differ the most are guluronate and mannuronate. Their basic structure is close to alginic acid **1** (Scheme 1), but the functional groups may be modified. Alginate gels used in biomedical applications are typically RGD-modified from alginic acid. RGD (arginylglycylaspartic acid) is a peptide motif responsible for cell adhesion to the ECM in the human body. The presence of RGD peptides makes alginate gels easier to control.[6,14]

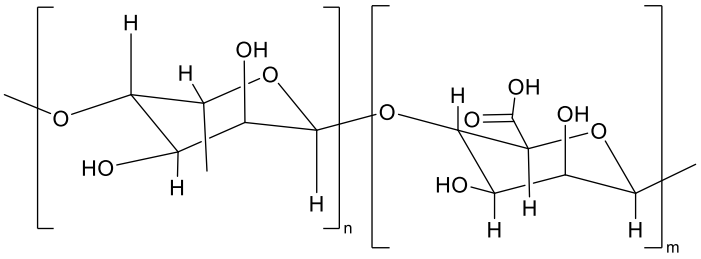

1

Scheme 1. The chemical structure of alginic acid polymer **1** from which alginate gels are modified.

Alginate is suitable for biomedical applications like cell culturing because of its biocompatibility, low toxicity, low cost, and mild gelation by the addition of divalent cations like Ca^{2+}. Products made from alginate are also orally administrated or injected into the body, giving various ways to apply. Alginate hydrogels are structurally similar to extracellular matrices of living tissue. The hydrogel is usually prepared using different cross-linking methods.[14]

The functionality of alginate can be modified. This can be done by changing the type of crosslinker and cross-linking methods. Depending on these factors, molecules can be released from alginate in a controlled manner. To improve physical properties, molecular weight can be changed. This affects the gel viscosity as higher molecular weight polymers have higher viscosity. Although alginate has low toxicity, it may include some harmful impurities, such as

heavy metals, proteins, and polyphenol compounds, as alginate is derived from natural sources. The impurities affect the immunogenic responses at injection or implantation sites. Luckily, these substances are easily removed via multi-step purification.[14]

2.1.4 Chitosan

Chitosan **2** is derived from chitin polysaccharide. Chitin has a crystalline structure due to its hydrogen bonding interactions between acetamide and hydroxyl groups. Chitin is unsuitable for use because it has a high number of acetylated groups, poor solubility to aqueous solutions and a rigid structure. Therefore, chitin is converted to chitosan via partial deacetylation, when it gains more amino groups and becomes more soluble in aqueous solutions. Biocompatibility and biodegradability are also enhanced.[11,15]

The polysaccharide structure of chitosan (Scheme 2) is constructed from glucosamine and *N*-acetylglucosamine. Chitosan is a weak base, and it can form hydrogen bonds that lead to the crystalline polymer structure due to the presence of amine and hydroxyl groups. Chitosan is biodegradable, and in the human body, degrading occurs naturally by lysozyme, acid, gastrointestinal enzymes, and colon bacteria. To use chitosan as a hydrogel, modification of its physiochemical properties is required. Typical modifications are stability and durability, which are done by polymeric cross-linking.[11,15]

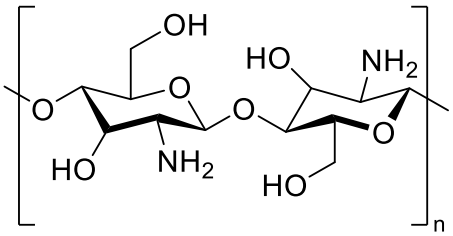

2

Scheme 2. The chemical structure of chitosan **2**.

2.1.5 Gelatin

Gelatin **3** (Scheme 3) is obtained from collagen by hydrolysis. Gelatin consists of multiple different functional groups. These functional groups allow it to host various cell lines because of suitable chemical and biological binding motifs to be used in cell culture. It is a good fit for biomedical research because it resembles ECM and its structural similarities.[11,16]

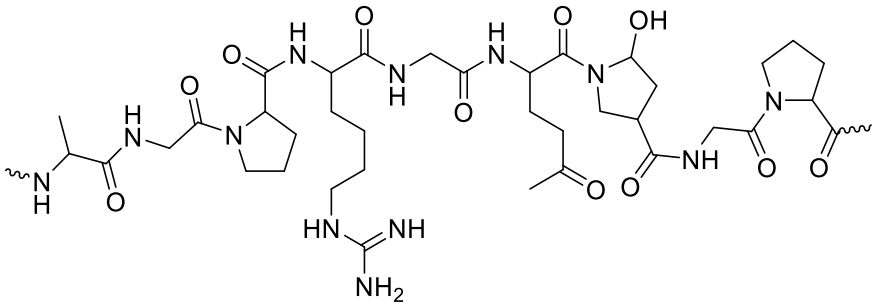

3

Scheme 3. The chemical structure of gelatin **3**.

Gelatin is considered a green and renewable material. In hydrogels, it is used because it gives consistency and viscosity. It is biocompatible, biodegradable, and non-toxic, and it is used for medical hydrogels because of its non-immunogenicity. It also has the capacity to enhance cell adhesion. Gelatin-based hydrogels are important for different applications, such as tissue engineering, drug delivery and environmental applications, such as removing pollutants from water.[16]

Gelatin has some limitations, like stability issues at high temperatures. This is caused by protein denaturation at temperatures above 40 °C. On top of this, gelatin is also water soluble, so if gelatin is synthesised to obtain neat material and not received from natural sources it causes problems in the purification of the synthesis products.[11,16]

2.1.6 Hyaluronic acid

Hyaluronic acid **4** (HA) is a polymer (Scheme 4) composed of disaccharides, gluconate, and *N*-acetyl glucosamine.[8] It is found in the human body as an immunoneutral polysaccharide and a crucial component for many cellular and tissue functions. HA is found in the natural ECM, where it contributes to the mechanical integrity of the network. HA is a good starting material for biomedical applications as it has the desired morphology, stiffness, and bioactivity. It is also suitable for the fabrication of artificial matrices because it is biocompatible, biodegradable, bioactive, non-immunogenic and non-thrombogenic.[17–19]

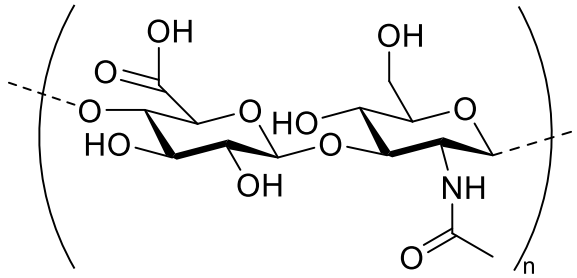

4

Scheme 4. The chemical structure of hyaluronic acid **4**.

In hydrogels, HA chains are randomly interconnected in macroscopic networks. This makes them unidentical to natural HA in ECM, which has more structural complexity and functional diversity. HA molecules contain multiple acid and hydroxyl groups, making them easy to modify chemically.[19] With studies made whilst combining cross-linking chemistries, scientists have successfully made alterations to the nanoscale and microscopic features of HA gels. These have made HA hydrogels better fitting to foster cell-matrix interactions. [17]

HA-based hydrogels are promising materials for tissue repair and regeneration as they are naturally involved in various cell signalling processes. HA has also been used in tumour studies because HA facilitates the migration of invasive tumours. This happens when HA interacts with certain cell surface receptors. To use in preclinical and clinical settings, HA can be chemically modified to physical forms like viscoelastic solutions, soft or stiff hydrogels, flexible sheets, and nanoparticulate fluids. HA derivatives obtained from living sources are required in 3D cell cultures and *in vivo* cell delivery. HA products that are traditionally extracted from animal sources suffer from batch-to-batch variations, such as varying molecular weight, the inhomogeneous gel and the existence of protein impurities that can be immunogenic. Another problem in using HA in cell and protein encapsulation is that covalent cross-linking of native HA requires toxic reagents.[17,18]

2.2 Synthetic hydrogels

Synthetic hydrogels are made of synthetic polymers or monomers via polymerization. These are, for example, polyethylene glycol (PEG) hydrogels, and polyacrylamide (PAM) hydrogels. Polymeric synthetic hydrogels are three-dimensional swelling networks of covalently or ionically cross-linked (like some natural hydrogels) hydrophilic homopolymers or copolymers hydrogels. They have better biomechanical properties than natural hydrogels, but they don´t have any inherent bioactivity. Also, the biggest problem is usually the toxicity of the material, as many syntheses might need toxic reagents to conduct the reactions.[5,7,20]

2.2.1 Polyacrylamide

Polyacrylamide **5** (PAM) is a synthetic polymer (Scheme 5) that has been used in molecular biology for a long time. PAM hydrogels are formed by a reaction of acrylamide monomer with bis-acrylamide crosslinker in the presence of ammonium persulfate (APS) and tetramethylethylenediamine (TEMED). APS is a source of free radicals and TEMED is a catalyst to initiate redox radical polymerization of the PAM.[8,11]

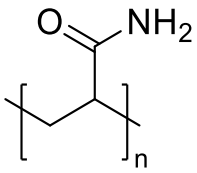

5

Scheme 5. The chemical structure of polyacrylamide **5**.

PAM is usually used in 2D studies where stiffness affects cell motility, spreading, and differentiation. Further interest in using PAM-based hydrogels in cell culture comes from the protocols used to fabricate the hydrogel. These advantages include the possibility of tuning the stiffness of the hydrogel very precisely, from less than one kPa to several MPa.[12] Another advantage is that it can be fabricated with coupling proteins. The changes in these two factors help to understand complex cell responses, that can't be accomplished with natural materials. The disadvantage of using PAM hydrogels is that the preparation of the hydrogels requires chemical crosslinkers that form free radicals (APS and TEMED). These free radicals cause cell toxicity, which makes the gel unsuitable for cell encapsulating uses. [8,11]

2.2.2 Polyethylene glycol (PEG)

Polyethylane glycol **6** (PEG) is a polymer (Scheme 6) with hydrophilic and relatively inert properties. PEG's basic structure is PEG diol with two hydrogen end groups. PEG can be cross-linked with different functional groups, such as methyloxyl, carboxyl, amine, thiol, vinyl sulfone, acetylene, and acrylate, making it applicable to many different uses. The two end groups can be symmetric (identical) or asymmetric (different). Due to this flexibility of use, PEG is used in cell culture applications like stem cell differentiation and angiogenesis.[11,21]

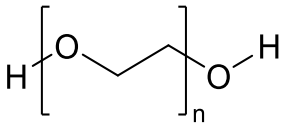

6

Scheme 6. The chemical structure of polyethylane glycol **6**.

PEG is mostly made via photopolymerization, which means that solid hydrogels of PEG monomers are achieved utilizing light. This cross-linking method is applicable for fabricating hydrogel scaffolds *in situ*, because it gives them spatial and temporal control. This makes them good scaffolds to provide 3D templates to apply in tissue regeneration.[21]

The disadvantage of using PEG hydrogels is that they have very limited biological activity, caused by the nonadhesive nature of PEG chains. Also, studies have shown that anchorage-dependent cells (adherent cells), cultured in PEG hydrogels have low viability due to PEG's bioinert characteristics. Luckily, bioactivity-modified PEG hydrogels have been developed to mimic ECM's proteins and polysaccharides. This can be done by adding RGD motifs.[11,21]

2.2.3 Polyvinyl alcohol (PVA)

Polyvinyl alcohol **7** (PVA) is a water-soluble and biocompatible synthetic polymer (Scheme 7), which contains many hydroxyl groups. PVA can form a hydrogel at room temperature when it's in a solution with a high alcohol percentage. The gelation density is not ideal with this method, so cross-linking methods (chemical and physical) are preferred to obtain a hydrogel with high mechanical strength, high water content, and good transparency. Cross-linking also strengthens and toughens the hydrogel.[12,22,23]

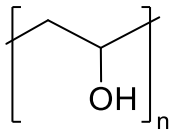

7

Scheme 7. The chemical structure of polyvinyl alcohol **7**.

The many applications of PVA hydrogels are, for example, 3D-printing tissue engineering material, self-healing gels, shape-memory materials, wearable electronic skin, and colorimetric sensors. [23] This huge variety of biomedical applications of PVA is caused by good modification properties due to the hydroxyl groups. This makes the mechanical properties easily improved. Also, the functionalisation of PVA results in changes in molecular weight that affect the degradation time (from less than a day to a month) and swelling rate of the hydrogel. The main disadvantage of PVA is that it shows only little adhesion to cell membrane proteins. Luckily, it is easily functionalised with esters, RGDs and photopolymerizable vinyl groups via hydroxyl groups. [12,22]

2.2.4 Dipeptide-based hydrogels

Dipeptides are small peptides that form hydrogels via molecular self-assembly and they have great importance in biomedical applications. They are constructed of amino acids which are attractive building blocks, have tunable mechanical properties, low production cost and synthetic feasibility. However, the design of dipeptide-based hydrogels is still challenging due to prediction difficulties caused by the complex nature of the molecular structure and hydrogel behaviour. Dipeptide-based hydrogels have been applied in drug delivery, tissue regeneration, 3D cell culture, and imaging.[24,25]

Dipeptides are constructed of a dipeptide part, formed of two amino acids. Amino acids have an amino terminus referred to as the N-terminus and a carboxyl terminus (-COOH) referred to as the C-terminus (Figure 4). The structure of the dipeptide hydrogelator allows it to be easily tuned, even with slight changes in structure. In nature, there are 20 different amino acids, all with different side chains. All 20 amino acids are not suitable hydrogelators and don´t show gelling abilities. Still, this gives dipeptide-based hydrogels significance in the self-assembled nanostructures.[25]

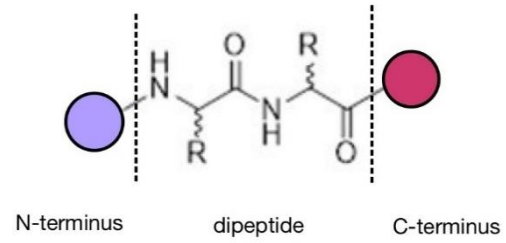

Figure 4. The core structure of a dipeptide hydrogelator.

Dipeptides self-assemble due to their non-covalent interactions, such as hydrogen bonding, electrostatic, van der Waals, π–π, and hydrophobic interactions. A clear pattern has not been observed between dipeptides' chemical structures and their associated hydrogel characteristics. Still, some machine learning and computational approaches have been used to predict gel formations based on peptides' two-dimensional chemical structures and self-assembly abilities.[24,26]

Some regularities are found to facilitate the design of dipeptide hydrogels. For example, Phe groups are a good choice for self-assembly in water as their hydrophobicity drives the self-assembly. The literature states that removing hydrophobic groups reduces the self-assembling possibilities of some hydrogelators. Chirality also plays a role in self-assembly, making it happen more easily when compounds are heterochiral. Still, self-assembly happens also with homochiral compounds. External and internal factors, such as solvent, temperature, light, molecular geometry and electronics, make molecular assembly difficult to predict.[25,27]

One way to divide the preparation of dipeptide gelators is based on the modification sites, like N-terminal modified dipeptide and C-terminal modified dipeptide. Adding a large aromatic group to the N-terminal of the dipeptide hydrogelator facilitates the self-assembly of peptides. Aromatic groups suitable for these modifications are fluorenylmethoxycarbonyl (Fmoc), naphthalene (Nap) derivatives, phenothiazine (PTZ), carboxybenzyl (Cbz), azobenzene (Azo), and pyrene (Pyr). Studies have shown that dipeptides without aromatic groups do not form hydrogels.[25]

The Fmoc group is the most widely used protecting group in peptide synthesis. Good hydrogelators containing Fmoc are commonly made by combining, glycine (Gly), alanine (Ala), leucine (Leu) and phenylalanine (Phe), such as Fmoc-Phe-Phe, Fmoc-Gly-Gly, Fmoc-Ala-Gly, Fmoc-Ala-Ala, Emoc-Phe-Gly and Fmoc-Leu-Gly. It is good to note that not all Fmoc-modified dipeptides form hydrogels in any conditions, or they form them at very low pH, which makes them unsuitable for biomedical applications. The good application ability of Fmoc has inspired to find other aromatic end groups, like naphthalene.[25]

The disadvantage is that these groups tend to be toxic, which makes them difficult to use in biomedical applications. Also, some challenges with biocompatibility exist. For, example the concentration needs to be low to be applicable. Therefore, the N-terminal can also be modified with non-aromatic groups, such as, hydrocarbonyl chain-modified dipeptides (C_n-dipeptides). These dipeptides have shown lower toxicity and better biocompatibility than those modified with Fmoc or Nap.[25]

Modifications made in the C-terminus are performed to disturb the hydrophobicity and hydrogen bonding capacity of the carboxylic acid moieties. These modifications have shown significant changes in self-assembling propensity, like the hydrogelation ability and morphology of hydrogel. Amide modifications have been observed to be more important than ester modifications, due to amides' extra hydrogen bonds. Also, adjusting the positions of the

added groups and the compound's sidechains can make a difference in dimensions making the nanostructures from 1D to 2D.[25]

2.3 Hybrid hydrogels

Hybrid hydrogels are formed by combining natural and synthetic hydrogels, which can make them more suitable for some applications, as they have positive elements of both natural and synthetic materials.[5] Hybrid hydrogels are composed of building blocks that are chemically, functionally, and morphologically distinct. The building blocks may include proteins, peptides, or nano/microstructures which are biologically active. These building blocks are interconnected physically or chemically. In addition, hybrid hydrogels are very heterogenic, which improves their cell adhesion, organization, and cell-cell interactions. Hybrid hydrogels expand the range of possible applications in biomedicine.[28]

Hybrid hydrogels are typically formed using polymers (synthetic or natural) as a base and then adding other structures to them.[28] When talking about natural polymers that work as a base of the hybrid hydrogel, we can categorise them into four main types: homopolysaccharides (e.g., cellulose), heteropolysaccharides (e.g., hyaluronic acid, chitosan), polypeptides/proteins (e.g., gelatin, collagen) and deoxyribonucleic acid (DNA) and ribonucleic acid (RNA). Hybrid hydrogels can also be made by combining two natural polymers to form protein/polysaccharide hybrid polymers like fibrin/cellulose, collagen/HA, gelatin/alginate etc. Synthetic polymers used in hybrid hydrogels can be classified into three types: non-biodegradable, biodegradable, and bioactive polymers. [29]

Homopolysaccharides and heteropolysaccharides are advantageous due to their biocompatibility and biodegradability. They are also applicable in similar areas like tissue engineering and wound dressing. Protein-based materials are advantageous for biomedical applications due to their similarity to mimicking extracellular environments. The most common application fields are more precise tissue engineering (with cartilage tissue and bone tissue) and drug delivery, as they degrade easily in the body. Common crosslinkers used are glutaraldehyde, formaldehyde and carbodiimide. DNA and RNA are less studied, but they still show very interesting possibilities for use in applications. They seem to be advantageous for biomedical applications due to their complexity and structural programmability.[29]

Hybrid hydrogels are prepared with different routes, such as cross-linking and processing methods. Cross-linking approaches can be physical cross-linking, chemical cross-linking, and irradiation cross-linking. Physical cross-linking is achieved with frequent freezing/thawing cycles leading to cryogels. Chemical cross-linking is done via cross-linking agents, such as borates, glyoxal, glutaraldehyde, etc. Irradiation cross-linking is based on irradiations, like electron beam or gamma radiation. The cross-linking modifications to the combined polymers can be done the same way as making natural or synthetic hydrogels. These modifications are chemical modifications to change ligands, functionalization of the surface by adding ligands, stealth functionalization, and PEGylation to increase the lifespan, which leads to improved bioavailability.[29,30]

Processing methods of hybrid hydrogels include solution casting/drying, theta gelation, methods related to freeze drying, inverse microemulsion polymerization technique, electrospinning, and coagulation treatment. New approaches to facilitate hydrogel self-assembly are click chemistry reactions, 3D printing, photo-patterning, and rapid prototyping.[29,30]

Table 1 presents, some examples of hybrid hydrogels constructed from natural and synthetic hydrogels presented in this thesis, their preparation methods, and medical applications found in the literature.[29]

Table 1. Examples of hybrid hydrogel compounds, their type, preparation methods, and medical applications

Natural polymer	**Synthetic components**	**Type of natural polymer**	**Preparation method**	**Applications**
Cellulose	PVA	Homopolysaccharides	Freezing/thawing cycles	2D-layered skin models
Cellulose nanocrystals	PAM	Homopolysaccharides	In situ polymerization	Scaffolds for tissue engineering
Cellulose nanocrystals	PAM and chitosan	Homopolysaccharides	Schiff base linkages and covalent cross-linking	Controlled drug release
Bacterial cellulose	PAM	Homopolysaccharides	Microwave irradiation	Oral drug delivery
Alginate	PVA	Heteropolysaccharides	Physical cross-linking	Scaffolds for cartilage tissue engineering
Chitosan	Benzaldehyde modified Pluronic	Heteropolysaccharides	Schiff base reaction	Drug delivery systems
HA	PEG	Heteropolysaccharides	Michael-type addition reaction	Cartilage tissue engineering
Gelatin	PEGDA	Polypeptides/proteins	Polymerization by light curing	Bone tissue engineering
Collagen	PVP (polyvinylpyrrolidone)	Polypeptides/proteins	Electrospinning	Artificial blood vessels
Gelatin	PPy (Polypyrrole)	Polypeptides/proteins	Polymerization	3D matrixes for nerve generation

3 Cell culture

Cell culture is an *in vitro* technique that aims to create an artificial environment for maximum cell propagation closest to the *in vivo* conditions. This is achieved by controlling the microenvironment where the cells are grown by changing factors like pH and temperature. Cell culture was invented in the early 20th century to study tissue growth and maturation in closed conditions to help virus biology and vaccine development.[31] Nowadays, it is an even more widely used technique that continues to develop new systems and applications.[32]

3.1 Preparing an appropriate microenvironment

The suitable artificial environment for cell growth includes a suitable culture medium which gives all needed nutrients (carbohydrates, vitamins, amino acids etc.) and can regulate the physiochemical environment (temperature, humidity, pH, O_2 and CO_2 tensions). Various culture medium compositions have been created to fill the requirements for different cell types (stem cells, nerve cells, bone cells etc.). The two main types of media used in research are natural and synthetic media. These mediums differ according to their supplemented serum. Serum's purpose is to provide the cells with growth factors and, hormones act as a carrier of lipids and enzymes and transport micronutrients. The serum is mainly used by adding it to the basal media.[31,32]

The desired temperature, pH, O_2 and CO_2 levels for the cell culture depend on the cell types used; for example, human and other mammalian cells differ. When human cells are grown, close to the normal body temperature (36-37 °C) and pH level around 7.2-7.4 is required if the target is to see how the cells would behave in humans or if the cell culture is later planned to be injected into humans. The pH is usually monitored by adding a pH indicator and kept stabile by a buffer. The O_2 and CO_2 must also be observed as they directly affect the growth speed if the metabolism is disturbed when the CO_2 balance changes.[32]

3.2 2D and 3D cell culture

Animal cells are preferably cultured either in 2D or 3D systems. Currently, most cells are cultured in 2D systems (Figure 5), based on growing cells on a flat surface, typically a petri dish made from glass or polystyrene. It has been used since the 1900s. Cell growth in 2D has all the same nutritional factors and growth rate as in medium, but in 2D, we can't control the cell shape the same way. There are a couple of methods to grow cells in 2D, such as so-called sandwich culture, micropatterning and altering substrate stiffness.[33,34]

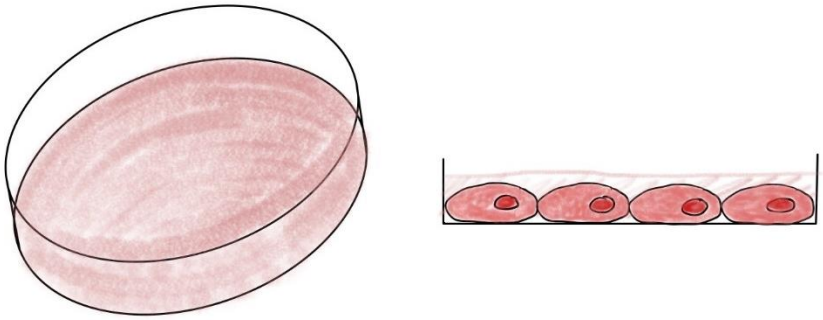

Figure 5. 2D cell culture shown in a petri dish as a flat surface and crosscut of the surface to show cells location in space.

2D culturing has problems mimicking the proper *in vivo* characteristics as it, for example, can't model some important characteristics of cancer cells.[33,34] To solve this problem, a three-dimensional (3D) cell culture (Figure 6) was created to mimic the *in vivo* conditions of cells better as they give an environment closer to the native one. [35]

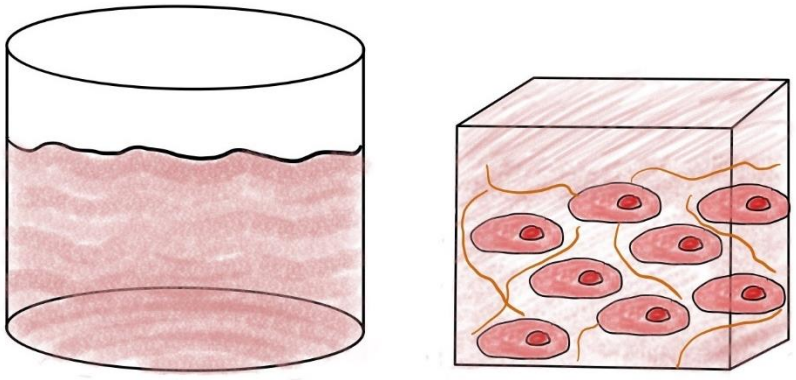

Figure 6. 3D cell culture shown as a thick layer and crosscut of the surface to show cells location in space.

The main difference between 2D and 3D culturing is that in 2D, the cells are grown on top of the gel surface and in 3D, they are grown inside the matrix material. This change of dimension affects many aspects, such as cell adhesion, spreading, polarity, cellular movement, and diffusion of proteins and small molecules.[12]

Hydrogels can be used as the base of cell culture systems. Depending on the hydrogel, it is important to consider whether culturing in 2D or 3D would be better. The type of experiment and cell to be studied determines whether to culture in 2D or 3D. Most cells modelled *in vivo* are best studied in 3D as the environment is closest to the natural matrix. Exceptions are also found, for example, epithelial and endothelial cells are closer to their natural environment in 2D models. Most hydrogels are suitable for both 2D and 3D culturing, but there might be some limitations, as some hydrogels might be too toxic for 3D culturing due to their precursor components.[8]

4 Hydrogels for cell culture

Classically, our knowledge of cell-based processes derives from 2D experiments performed on flat, physiologically stiff materials like polystyrene and glass. These surfaces are not ideal as they usually result in abnormal results like flattened shape and altered response to pharmaceutical reagents. So logically, these systems do not perfectly represent the three dimensions of cells affecting in the human body. New biomaterial systems have been made to improve culture systems, so they better mimic the actual biological systems and give answers to the wanted gaps in conventional cultures. They also help to understand native *in vivo* systems.[8,12]

Hydrogels have shown the best results from these biomaterial systems to culture cells. The hydrogels' water-swollen polymer network mimics the salient elements of native ECMs, has mechanical properties similar to soft tissues, and they can support cell adhesion and protein sequestration. Because of these properties, hydrogels are used as models to solve problems facing drug screening, cancer treatment, tissue engineering etc.[8,12]

While applying a hydrogel for cell culture, the capacity to mimic cells' natural environment is essential. Factors like stiffness, porosity, and biodegradability can make a huge difference in the usability of the hydrogel. The stiffness of the ECM affects regulating adhesion, migration, differentiation, and more. The stiffness of hydrogel can be controlled by polymer concentration or cross-linking density. The desired stiffness depends on the cells used. For example, optimal stiffness for brain tissue is as low as 0.1-1 kPa, whereas for muscle tissue, 8-17 kPa is optimal. Adding the cells to the matrix can make the hydrogel stiffen more or rupture the structure because of added stress.[12]

Biodegradability is a critical condition to hydrogel design when applied in biomedical areas. When biomedical products are consumed, they go through digestion and metabolism and break down. Examples of degradation processes are solubilization and hydrolysis of biological entities of hydrogels. Therefore, the degradation by-products need to be harmless. In hydrogels, biodegradability is determined by the by-products formed from hydrogen breaking and the hydrogel preparation method. Hydrophilic, natural, and synthetic polymers are examples of biodegradable polymers. Factors like temperature and pH, can affect the hydrogel breakdown by solubilization. Not all polymers are decomposed by simple hydrolysis, but via chemical hydrolysis or enzyme hydrolysis.[5]

The porosity of the material is an important factor for cell viability. Hydrogels usually contain both small and large pores. The porosity affects the transportation of nutrients, carbon dioxide and oxygen, and even small changes in pore size on the nanometre scale are distinguishable by the cells. The porosity of hydrogels can be studied, for example, with MIP (mercury intrusion porosimetry) and SEM (scanning electron microscopy) techniques and controlled on the microscale by using solvent phase inversion and on the macroscale by encapsulating inorganic particles.[12,20]

For using hydrogels in applications, their properties and their processing requirements must be considered.[20] Table 2 summarises the hydrogels discussed in Chapter 2, with their advantages, disadvantages, and most common applications.

Table 2. Examples of hydrogels and their applications

Hydrogel	**Nat./Synth.**	**Advantage**	**Disadvantage**	**Applications**
Collagen	Natural	Good collagen-to-cell ligand binding	Poor mechanical properties	Drug delivery, tissue engineering
Fibrin	Natural	Contains naturally cell binding sites, ECM proteins and growth factors	Weak mechanical properties that make it unsuitable for bone tissue engineering	Nerve repair
Alginate	Natural	Biocompatibility, low toxicity, and low cost	Poor viscosity	Injectable medicine
Gelatin	Natural	Structural similarities to ECM, availability, cost-effectiveness, excellent biodegradability, and biocompatibility	Poor stiffness	Tissue engineering, drug delivery
Chitosan	Natural	Crystalline polymer structure with the presence of amine and hydroxyl groups	Weak stability and durability	Wound healing
Hyaluronic acid	Natural	Naturally found in ECM	Poor mechanical properties	Tissue repair and regeneration, tumour studies
PAM	Synthetic	Good stiffness tuning abilities	Preparation requires chemical crosslinkers with free radicals	2D cell culture
PEG	Synthetic	Good hydrophilic properties and cross-likability	Limited in their biological activity	Goo scaffolds to 3D tissue regeneration
PVA	Synthetic	Water soluble and biocompatible, with many hydroxyl groups	Little adhesion to cell membrane proteins	3D printing, self-healing gels
Dipeptide	Synthetic	Wide range of possibilities for modifications	Tendency of toxicity	Various

5 Applications

Hydrogels can be used in many biomedical applications, some of which are presented in Figure 7. Here applications are presented from the point of view of previously presented hydrogels for cell culturing. For many biomedical applications, cell culture is an important and necessary process.[34]

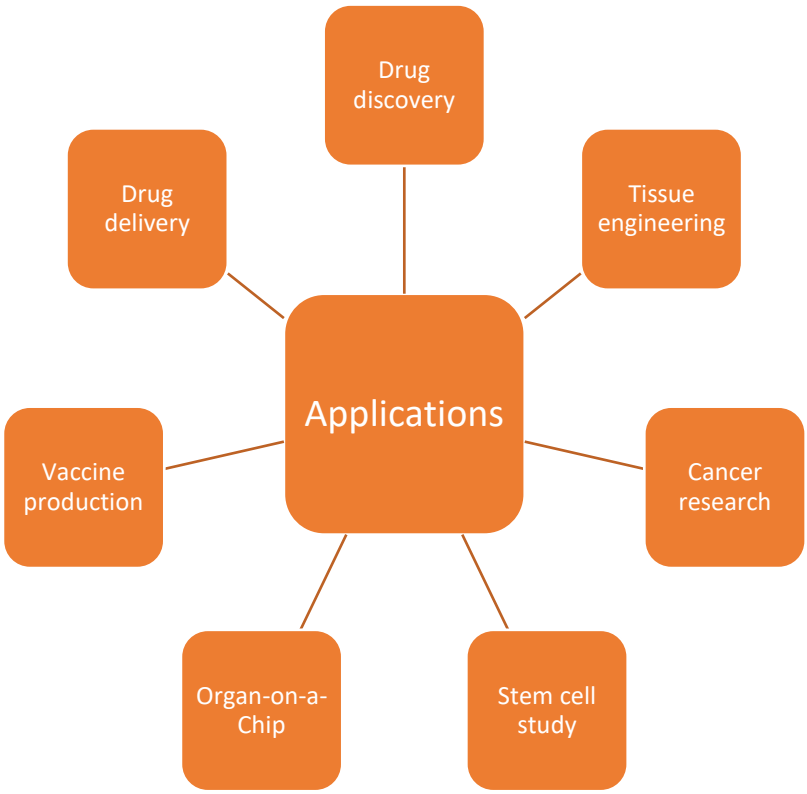

Figure 7. Biomedical applications of hydrogels

5.1 Drug discovery

Drug discovery is one of the most important fields of study in medicine and pharmacology. The process of drug discovery (Figure 8) starts from Early drug discovery (Stage 1), Pre-Clinical phase (Stage 2), Clinical phase (Stage 3) and Regulatory approval (Stage 4). Clinical phase is composed of three phases: Phase I, II, and III. The studies have lowest success rate in Phase II and Phase III. Problems with drug discovery is that it is time consuming and expensive, as very few drugs pass the clinical trials. Nowadays, 2D cell cultures are most used methods in drug discovery, especially in Pre-Clinical trials to test drugs processing in cell like material. 2D cultures manage to mimic biological processes well, but they lack some complicated microenvironmental processes. This is battled with understanding the link between cells and the ECM.[34,36]

Figure 8. Drug discovery process and where hydrogels are needed

Cell cultures have also been done in 3D to test drugs. The responses of the cells in 2D and 3D cultures have differed in physical and physiological properties. 2D cells are more sensitive to drugs than 3D cells due to the different organisations of surface receptors. This is because drugs target certain receptors for cell surfaces to effect. Also, cells cultured in 2D are more homogenous as the cells grow in the same stages, unlike in 3D cultures. In 3D cultures, cell stages can vary, resembling closer *in vivo* cells. Differences in cell stage cause proliferation on the outer parts, which is necessary for many drugs to be effective. pH levels differ also between 2D and 3D. From the point of view of metabolism, 3D cultures mimic natural pH levels better than 2D culture models. Due to these reasons, 3D cell culture has become the top method in drug discovery because 3D cell culture allows cell-to-cell and cell-to-matrix interactions to be observed.[34]

5.2 Drug delivery

Controlled drug delivery systems aim for efficient drug delivery in the body. In drug delivery research, hydrogel's ability to release medicines in a controlled manner and long period of time is advantageous. The extended-release time makes the medicine active for a long time.[5]

Physical (electrostatic interactions) and chemical (covalent) approaches can be used to increase the binding between the loaded drug and hydrogel matrix and extend the drug release time. Therefore, hydrogels can store certain medications from harsh conditions and release them at the right kinetics. Variations in pH, temperature, light, magnetic or electric field, ionic changes and pressure can be used as stimulus to cause the drug release. Hydrogel networks (Figure 9) store water molecules inside the network by connecting to hydrophilic groups of the network. When a stimulus activates the swollen network, swelling and shrinking of hydrogel happens, resulting in the drug release.[5,37]

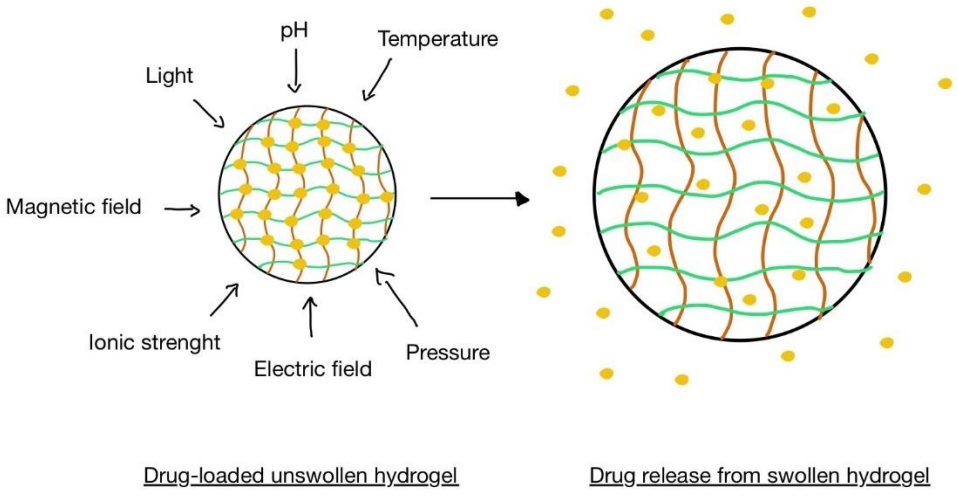

Figure 9. Drug delivery from the unswollen hydrogel network, when irritated with stimulus to activate the swelling of hydrogel and later releasing the drug. Yellow dots represent drug molecules, and the green and brown lanes represent the wavy matrix structure.

5.3 Organ-on-a-chip model

Organ-on-a-chip models have been developed to perform experiments where a 3D microfluid system mimics a cell´s microenvironment via a hydrogel scaffold. Microtechnology-based hydrogels can provide tissue-specific information about the delivery of chemicals, nutrients, and oxygen. Therefore, hydrogels are used in organ chips as a ECM barrier to analyse cell to ECM interactions. These factors give us more accurate information for the prediction and analysis of cellular responses in relation to drugs and therapeutic agents. Various models have been developed based on these principles, including gut, liver, skin and vasculature models.[34,38]

Organ-on-a-chips (Figure 10), also called organ chips, are created by fabricating a microchip with a computer and then populating it with living cells. These living cells resemble *in vivo* organ-level physiology and pathophysiology. This is made possible by constructing tissue-level and organ-level structures. Organ chip models permit high-resolution and real-time imaging making it easy to analyse *in vitro* biochemical, genetic, and metabolic activities presented in tissue.[34]

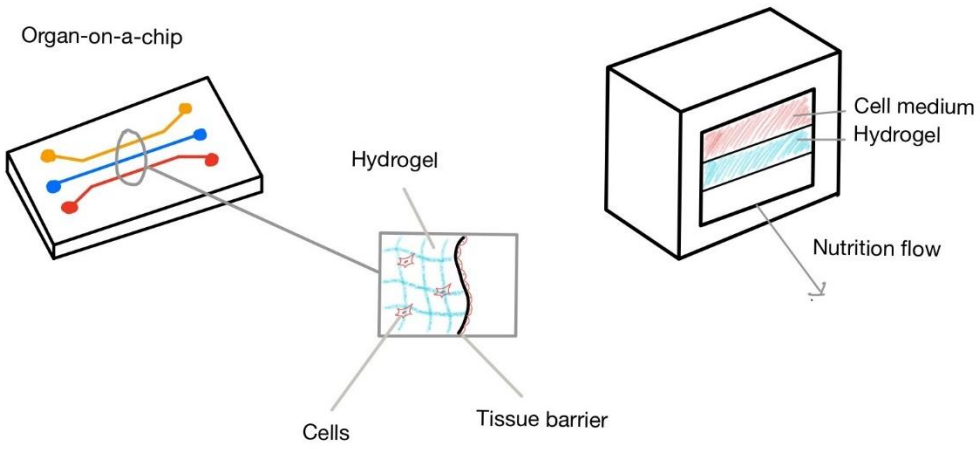

Figure 10. Organ-on-a-chip cross-section to show hydrogels place in the chip. Hydrogel works here as ECM barrier, and it is used to mimic cell ECM interactions.

Some organs have been successfully modelled with organ chip models like, kidney tubules, small intestines, liver, and bone marrow. These models have also shown accurate organ-level responses to stimuli like drugs, toxins and pathogens. For example, gelatin can be used as a coating in organ-on-a-chip applications.[11] Even more complex models, such as human-on-a-chip models, have been envisioned to examine human physiology more completely. Therefore, organ chip models are a promising application for hydrogels.[34]

5.4 Tissue engineering

Tissue engineering is a field of study which combines life science, biochemistry, and engineering to form a wide understanding of the structure and function of tissue. It searches for synthetic substitutes that mimic the tissues found in the human body to be applicable in repairing damaged tissue or organs. Tissue engineering also gives answers to problems facing organ donation. An important process used in tissue engineering is 3D cell culture-based research and development. [14,39]

The tissue engineering process (Figure 11) starts with a biopsy off the damaged tissue. After the biopsy, cells are isolated, cultivated, and proliferated, then contacted with scaffolds, and the tissue development starts. The 3D scaffolds are produced from natural polymers, such as hydrogels. When the tissue has been grown, the implantation of the product can be done back to the patient.[40]

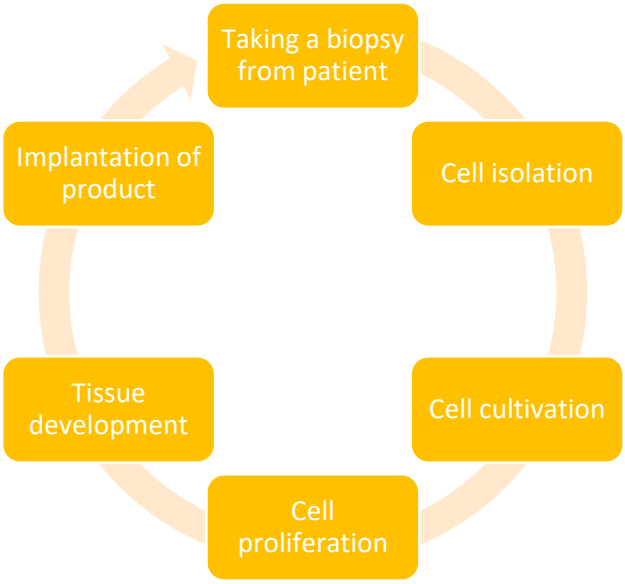

Figure 11. Process of tissue engineering.

Natural hydrogels like alginate gels are promising for tissue engineering. In tissue engineering hydrogels are used as scaffolds to provide a space for new tissue formation, deliver cells to the desired site, and control the structure and function.[14] These scaffolds can be produced in 3D cell cultures via various methods like freeze-drying, solvent casting particulate leaching, electrospinning, and 3D printing. Freeze-drying id based on rapid cooling of the solution, producing a scaffold with a porosity of more than 90% and pore size from 20 to 200 µm. Solvent casting particulate leaching creates scaffolds by mixing water-soluble salt particles into a biodegradable polymer. When the salt particles are removed, a porous structure is obtained. Electrospinning utilises an electric field to form polymer fibres onto a specific substrate. 3D printing allows designing scaffolds with computers and printing them. [34]

In tissue engineering, the human organs can be divided into four categories for *in vitro* organ development based on their structure complexity: zero complexity fat structures (e.g., skin), tubular structure (e.g., blood vessels), hollow organs (e.g., stomach), and solid organs (e.g., heart). The development of organoids on hydrogel scaffolds has been challenging as they lack vascularization. This brings other limitations like small size, slow proliferation rate, lack of immune system and limited growth. Therefore, it is important to set vascular structures in organoids. Various approaches like additive manufacturing (e.g., bioprinting), sacrificial networks, subtractive fabrication, and spontaneous vascularization have been adopted to develop vascularized organoids. Another approach is micro-fabrication techniques which have enabled the development of size-controlled vascularized organoids.[39]

5.5 Stem cell studies

Stem cell studies are used in cell therapy applications. In clinical applications, 2D cell culture techniques have proven to be ineffective when using stem cells. This is caused by the inaccuracy of the *in vivo* microenvironment of 2D models. Also, the low cell retention rates of stem cells *in vivo* cause problems. To improve cell viability, biomaterials, such as hydrogels, to encapsulate cells before their transplantation have been used.[34,41]

Some hydrogels like PEG have already been used cell culture applications facing stem cell differentiation.[11] Still, more hydrogels must be studied for stem cell studies, as PEG is not suitable for all applications. When studying hydrogels, it is important to consider stem cells´ mechanical and material properties, like bulk stiffness. Stiffness, biodegradability, morphology, and by-products are known to play a role in stem cell differentiation and proliferation. However, the exact ECM factors remain difficult to identify. An ideal hydrogel for stem cell studies will degrade completely and allows cells to proliferate simultaneously.[41]

5.6 Tumour and cancer studies

Understanding the characteristics of tumours is important for understanding various cancer types.[34] Tissue engineering principles have been applied to the fabrication of 3D tumour tissue. Studies utilizing these *in vitro* models can produce better knowledge of tumour biology. HA is naturally highly expressed in tumours, so it is an interesting hydrogel to study from this aspect.[17]

Traditional cancer treatments, like chemotherapy are very burdensome for the whole body. Therefore, targeted drugs directly delivered to the cancerous tumour area with the help of hydrogels would be beneficial. The drugs can be included in the cross-linked 3D networks of polymeric chains to enable drug delivery to the target tumour cells. Modified drugs could be inserted into the desired place with injectable hydrogels.[5]

Tumour models can also be used in studies observing cellular signalling pathways. These cellular pathways can be mapped and then compared to 2D cultured cell models to determine if the models are viable or not. If the 2D model does not match the 3D *in vivo*-like model, it can be assumed that pathways in the 2D model are inaccurate. On top of that, tumour-on-a-chip models have also been invented. These are like organ-on-a-chip models, but they grow tumour cells on the chip.[34]

5.7 Vaccine production

For proper immunization, the appropriate delivery of vaccines is a significant factor. This requires proper delivery of antigen to the right place where it responds along with a stimulus starting an immune response. The vaccine delivery system aims to slowly release and deliver antigen molecules, so booster shots are not required. Polymeric hydrogel-based vaccine delivery systems have shown proper applicability with desired functions. These systems are unique, and they have several advantages. They can provide an alternative method of needle-based vaccines and can stimulate the antigen-mediated immune response. As hydrogel-based systems can be prepared with biocompatible polymers, polymers within the hydrogel can undergo degradation within the physiological system.[42]

The efficiency of vaccine delivery systems relies on appropriate immune response establishment of immunological memory. In theory, the closer the vaccine is delivered to the lymph node or lymphatic vessel, the stronger the immune response is. Vaccine delivery systems made of synthetic or natural polymers facilitate the releasing environment through site-specific degradation and create a suitable platform for efficient vaccine delivery. Hydrogel-based systems base their functionality on encapsulating vaccine molecules and releasing them upon entering the animal or human body.[42]

Nowadays, a variety of vaccine delivery systems are based on hydrogels (Figure 12). All these systems respond to certain needs and problems facing vaccine production. For example, not all vaccines need to be or can be injected to the target, so orally taken bio bullets are an excellent response to this.[42]

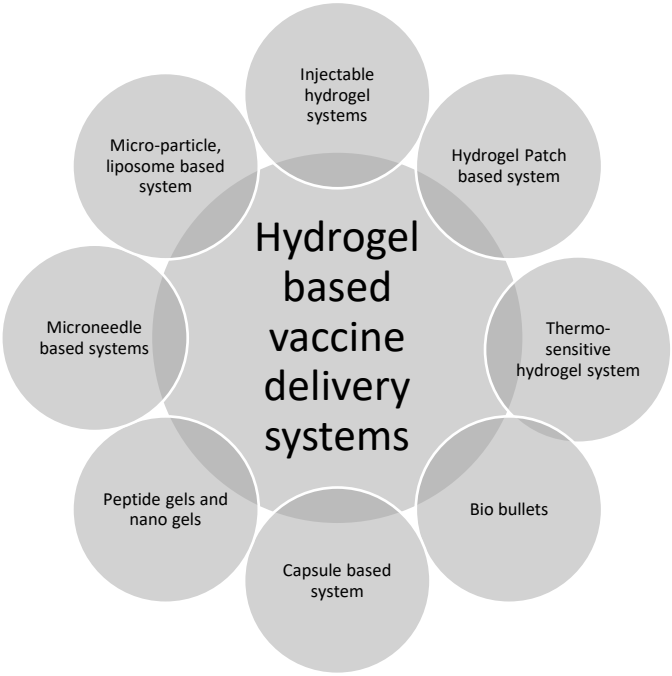

Figure 12. Hydrogel-based vaccine delivery systems.

5.8 Other applications

There are many other applications of hydrogels in biomedicine, but they are not yet as studied, or their applications are still on a very novel level. Some mentionable applications are neuronal growth[43], injectable hydrogels[24] and wound healing[5].

An interesting topic to study in tissue engineering is neural cell cultures. Both synthetic and natural hydrogels can be used as scaffolds in these studies. For neuron studies, very soft tissues in the range of 0.5 to 2.5 kPa are required as the brain is a soft material. A study conducted with the self-assembling of alkyl galactonamides proved suitable for 3D cell culture of neuronal cells.[43] These hydrogels formed long ribbon-like fibres which reach hundreds of micrometres in length and several micrometres in width. The entanglement of ribbon-like fibre is loose, which provides large and open interspace for cells to migrate and grow in 3D. [43]

Injectable hydrogels can be used in drug delivery, wound healing, and tissue engineering.[24] Conventionally, transplantation of hydrogel requires surgery. For this reason, injectable hydrogels are a good solution as they are in the sol phase outside the body and then convert into the gel phase upon injection. The sol-gel transition of hydrogel needs to be made via cross-linking of injected polymer chains caused by external stimuli, such as light, temperature, pH, electric and magnetic fields, ionic strength, or shear force. The desired features for an injectable hydrogel are stiffness, stretchability, adhesiveness, antimicrobial activity, conductivity, and self-healing.[7]

Hydrogels can also be applied in wound healing as they are insoluble polymers with a high water content of over 90%. Due to this, the hydrogel can provide water to the wound site, making the environment moist. The theory behind hydrogel hydration abilities has been linked to the presence of groups like -OH, -COOH, -$COHN_2$, -COHN-, and -SO_3H. Another positive factor of hydrogels is that they show significant protection against microbial attacks. Polymers that seem promising to hydrogels of this kind are for example, alginate, chitosan, gelatin and PEG.[5]

Other mentionable applications are biosensors, spinal cord regeneration, bone regeneration, anti-fungal and anti-bacterial applications, self-healing hydrogels, and hydrogels-based sensors. Hydrogels are also used in contact lenses and hygiene products, but methods do not rely on cell culturing, so they are not discussed further in this thesis. The long list shows that the applicability of hydrogels in cell culture-based applications is almost limitless. More studies are needed to nail the optimal application and usability.[5,7]

6 Summary

The literature part presented the applicability of hydrogels in cell culture applications. Cell culture is an *in vitro* technique that aims to create an artificial environment, with animal cells either in 2D or 3D systems. Cell culture is important to help us understand biological processes happening in the human body on the cell levels. Hydrogels are a good use in cell culture applications, because their water-swollen networks mimic complex structures of actual cells. The favoured qualities are a salient element of ECMs, mechanical similarities to soft tissues and support of cell adhesion and protein sequestration.[8]

Hydrogels used in cell culture needs to be precisely chosen. Different hydrogels, natural, synthetic, hybrid, have all different advantages and disadvantages. This lies on the capacity to mimic cells' natural environment on a wanted purpose. Factors like stiffness, porosity, and biodegradability all change the usability of the hydrogel. The desired stiffness depends on the cells used, and it can be controlled by polymer concentration or cross-linking density. Biodegradability needs to be considered as some biomedical products are consumed, so they go through digestion and metabolism. Therefore, the degradation of by-products needs to be studied. The porosity affects cell viability by the transportation of nutrients, carbon dioxide and oxygen. Fabrications to the porosity are made either on the macro-scale or micro-scale. [5,12,20]

Applications of hydrogels in biomedicine related to cell cultures are almost limitless. For many biomedical applications, cell culture is an important and necessary process. Some, biomedical applications that rely on cell culturing are drug discovery, drug delivery, organ-on-a-chip model, tissue engineering, stem cell studies, tumour and cancer studies, and vaccine production. On top of these there are still many possible applications, but they are less studied, and they lack successful results. Still, biomedical applications of hydrogels are a growing field which makes them an interesting subject to study.[5,34]

EXPERIMENTAL PART

7 Aim of the study

The aim of the study was to prepare two known hydrogelators and then compare their gelling properties. The prepared gelators (Scheme 8) were FmocFFCOOH and CinFFCOOH dipeptides. The CinFFCOOH was prepared according to previous studies.[2] The current work consisted of six synthetic steps, two for synthesising dipeptide FmocFFCOOH and four for preparing dipeptide CinFFCOOH. Due to the limited time and lack of pure CinFFCOOH product, the gelation comparison of these two compounds was not performed. However, the gelation behaviour of FmocFFCOOH was assessed.

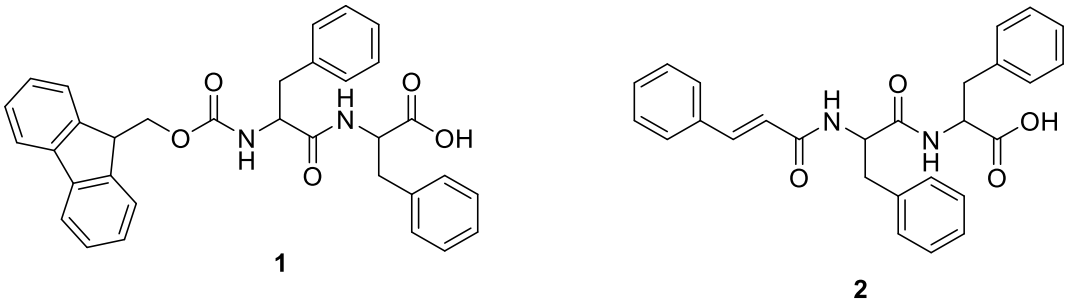

Scheme 8. The chemical structure of dipeptides FmocFFCOOH **1** and CinFFCOOH **2**.

8 Research methods

8.1 Chemicals

All chemicals (Table 3) were used without further purification. The chemicals were weighed using the Metler Toledo XP205 scale, and the Denver Instrument APX-200 scale was used to weigh round-bottom flasks.

Table 3. List of used chemicals, manufacturers, and their purities

Chemical	**Manufacturer**	**Purity (%)**
Cinnamic acid	Fluka	> 99.0
Dichloromethane	VWR Chemicals	-
Diethyl ether	VWR Chemicals	-
Dimethylsulfoxide-d_6	Eurisotop	99.80
Ethyl acetate	VWR Chemicals	-
Fmoc-L-Phe-L-Phe-OH	Abcr	95.0
Hydrochloric acid	VWR Chemicals	37.0
Hexane	Honeywell	-
Magnesium sulfate hydrate	Fluka	-
Methanol	Honeywell	> 99.8
N-[(9H-Fluoren-9-ylmethoxy)-carbonyl]-L-phenylalanine	TCI	> 98.0
N-(*tert*-Butoxycarbonyl)-L-phenylalanine	TCI	> 99.0
N,*N*-Dimethylformamide	Acros Organics	99.8
Sodium hydrogen carbonate	VWR Chemicals	-
(*S*)-3-Phenylalanine t-butyl ester HCl	Biosynth	-
Sulfuric acid	Fluka	95.0-97.0
TBTU	Fluorochem	> 98.0
tert-butyl acetate	TCI	> 99.0
tert-butyl Methyl Ether	TCI	> 99.0
Toluene	VWR Chemicals	-
Trifluoroacetic acid	Apollo Scientific Limited	99.5

8.2 Instruments

Used equipment is listed below with their details.

NMR spectroscopy: ^{1}H and ^{13}C NMR spectra were measured with Bruker Advance III HD 300MHz spectrometer and 500MHz spectrometer.

FTIR spectroscopy: A Bruker Alpha FTIR spectrometer was used to record all FTIR spectra. The used spectral range was 4000-400 cm^{-1}.

HR-MS: Agilent 6560 was used to measure high-resolution mass spectra (HR-MS).

Evaporator: The Heidolph Laborota 4000 efficient evaporator was used to evaporate the solvents.

Sonicators: Two sonicators were employed, the UP50H Ultrasonic Processor, Hielscher, Ultrasound Technology (Cycle 1, Amplitude-% 100) and the Elmasonic S, Elma sonicator water bath.

9 Experimental methods

9.1 Synthetic protocols for FmocFFCOOH 1

9.1.1 Synthesis of FmocFFO*t*Bu 3

The synthesis for FmocFFO*t*Bu **3** is given in Scheme 9.

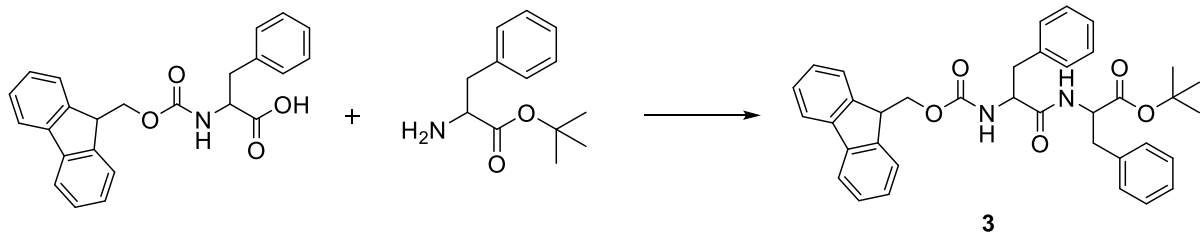

Scheme 9. The chemical reaction for the formation of FmocFFO*t*Bu **3**.

FmocF (1.0g, 1.0eq), FO*t*Bu (0.732g, 1.1eq), TBTU (0.829g, 1.0eq) and $NaHCO_3$ (0.239g, 1.1eq) were added to anhydrous DMF (20ml) under N_2 atmosphere at RT. The solution was left to stir overnight under the same conditions. The next day a TLC (Hexane (Hex): Ethyl acetate (EA), 1:1, Hanessian's stain) confirmed the consumption of the starting materials. The solvent was evaporated by co-evaporation with toluene (x3). The residue was dissolved in DCM and then extracted with water (x2), and subsequently washed with HCl 0,1M (x2), water (x2) and saturated aqueous solution of $NaHCO_3$. The organic phase was dried with $MgSO_4$, evaporated to dryness, and then dried under vacuum. A white glassy solid was produced at a 31% yield (0.4654g).

To prove the purity, we measured NMR and HR-MS spectra. The ^1H (Figure 13) and ^{13}C (Figure 14) NMR spectra of FmocFFO*t*Bu agree with previously published data.[44] The corresponding functional groups/moieties are highlighted in bold letters in all ^1H NMR chemical shifts.

^{1}H NMR (300 MHz, DMSO) δ 8.35 (d, *J* = 7.4 Hz, 1H, N**H**), 7.86 (t, *J* = 8.4 Hz, 2H, **Ar**), 7.62-7.55 (m, 3H, **Ar**, N**H**), 7.39 (dd, *J* = 15.9, 8.5 Hz, 2H, **Ar**), 7.34 – 7.15 (m, 12H, **Ar**), 4.48 – 4.24 (m, 2H, C**H**), 4.19 – 3.98 (m, 3H, **Fmoc**), 3.06 – 2.87 (m, 3H, **Phe**), 2.75 (dd, *J* = 16.8, 7.5 Hz, 1H, **Phe**), 1.31 (s, 9H, ***t*Bu**).

^{13}C NMR (75 MHz, DMSO) δ 171.57, 170.32, 155.68, 143.73, 143.67, 140.61, 138.06, 137.05, 129.17, 128.11, 127.96, 127.56, 126.99, 126.45, 126.19, 125.29, 125.20, 121.33, 120.02, 80.84, 80.63, 65.61, 55.79, 54.18, 46.50, 38.20, 37.42, 36.77, 27.47.

HRMS (ESI-TOF, m/z) calculated for $C_{37}H_{38}N_2O_5$ $[M + Na]^+$ 613.26, found 613.2659 (Appendix 1).

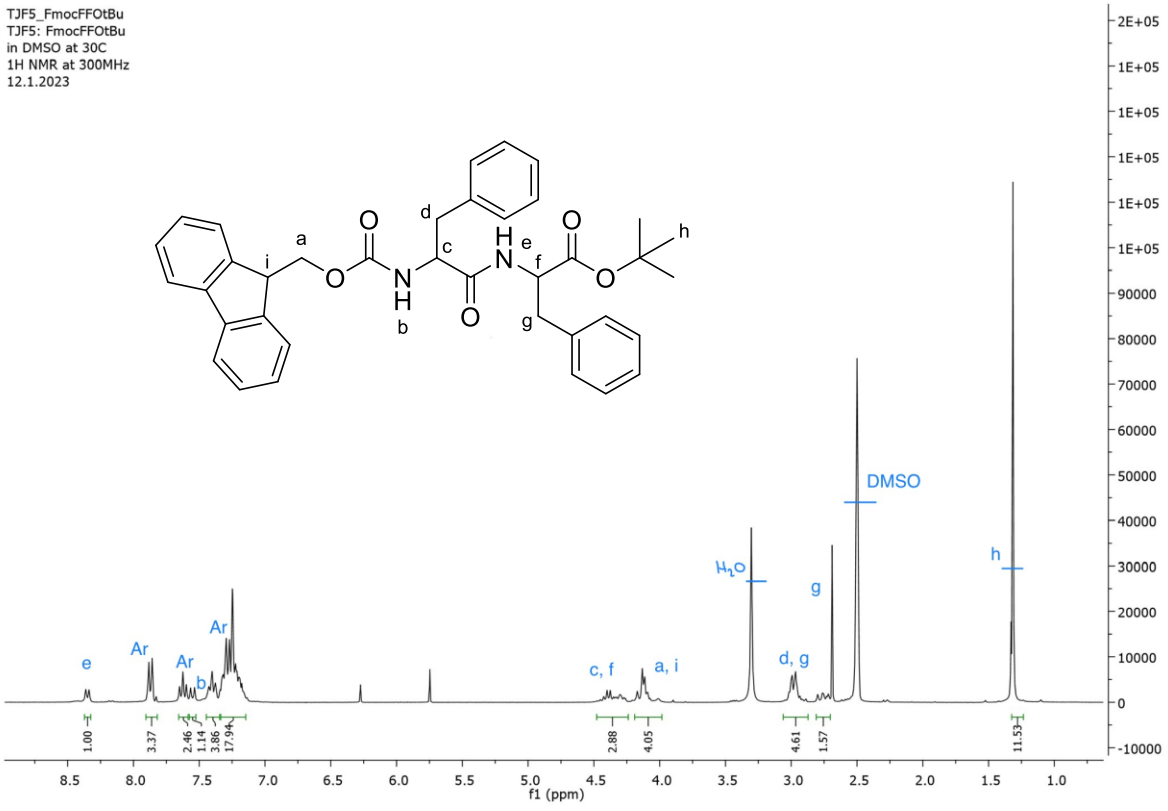

Figure 13. ^{1}H NMR (300 MHz, d_6-DMSO) spectrum of FmocFFO*t*Bu.

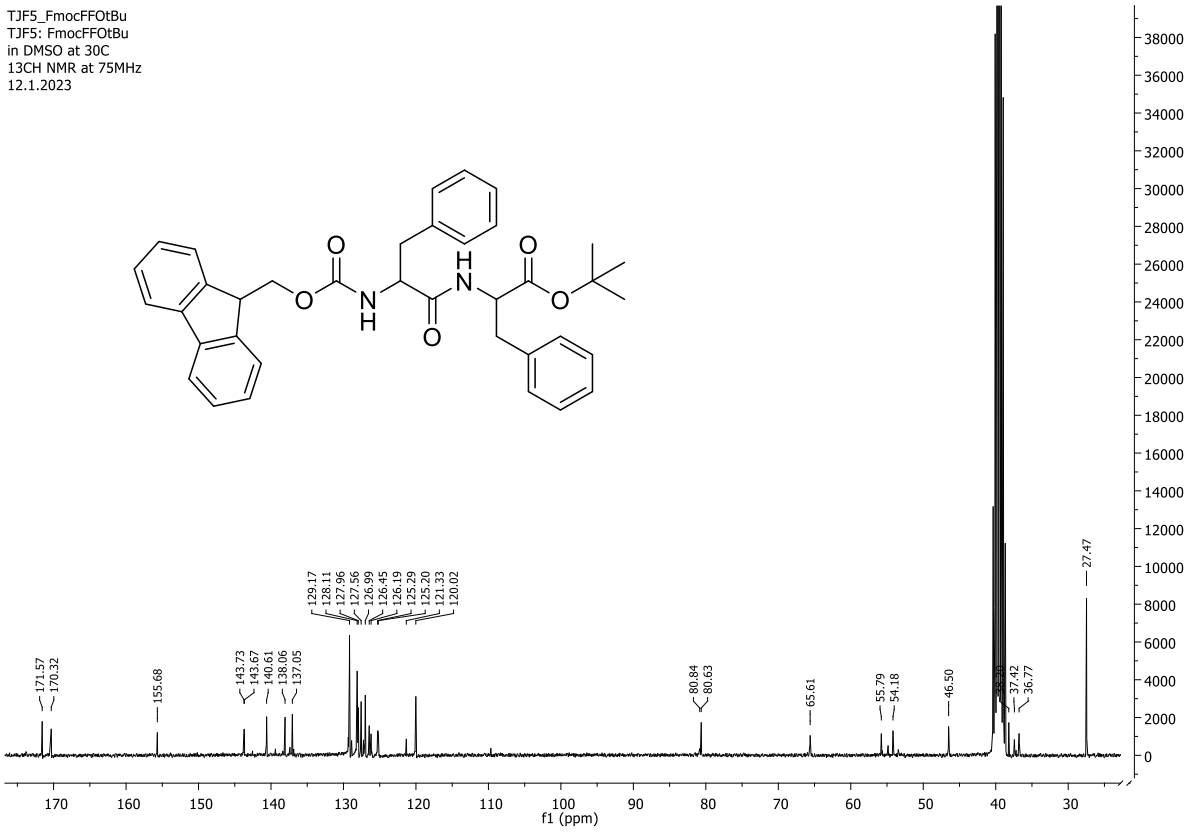

Figure 14. ^{13}C NMR (75 MHz, d_6-DMSO) spectrum of FmocFFO*t*Bu.

9.1.2. Synthesis of FmocFFCOOH 1

FmocFFCOOH **1** was prepared from FmocFFO*t*Bu **3** according to the reaction shown in Scheme 10.

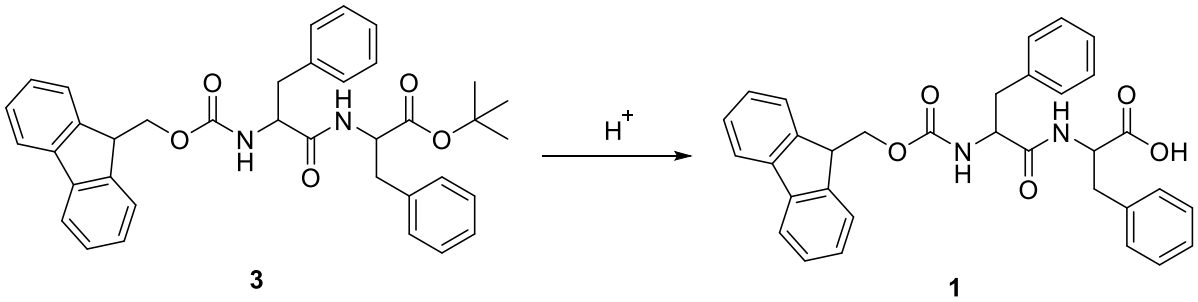

Scheme 10. The deprotection reaction of FmocFFO*t*Bu **3** towards FmocFFCOOH **1**.

FmocFFO*t*Bu (0.465g, 1.0eq) was dissolved in DCM (1.3 ml). TFA (1.3 ml) was added to the solution and the reaction was left to stir for 1h at RT. TLC (EtOAc, Hanessian´s stain) verified the consumption of all starting material. The reaction mixture was then co-evaporated multiple times under vacuum with DCM. A white solid formed, which was then mixed with diethyl ether and filtrated. The obtained solid was left to dry overnight under vacuum (0.2486 g, in stoichiometric yield).

To prove the purity, we measured NMR and HR-MS spectra. The ^{1}H (Figure 15) and ^{13}C (Figure 16) NMR spectra of FmocFFCOOH agree with previously published data.[44] The corresponding functional groups/moieties are highlighted in bold letters in all ^{1}H NMR chemical shifts.

^{1}H NMR (300 MHz, DMSO) δ 8.24 (d, J = 7.8 Hz, 1H, N**H**), 7.87 (d, J = 7.5 Hz, 2H, **Ar**), 7.62 (t, J = 7.0 Hz, 2H, **Ar**), 7.54 (d, J = 8.9 Hz, 1H, N**H**), 7.40 (t, J = 7.5 Hz, 2H, **Ar**), 7.34 – 7.14 (m, 12H, **Ar**), 4.49 (dd, J = 13.3, 8.1 Hz, 1H, C**H**), 4.33 – 4.24 (m, 1H, C**H**), 4.18 – 4.07 (m, 3H, **Fmoc**), 3.09 (dd, J = 13.9, 5.3 Hz, 1H, **Phe**), 2.96 (dt, J = 13.9, 6.9 Hz, 2H, **Phe**), 2.79 – 2.68 (m, 1H, **Phe**).

^{13}C NMR (75 MHz, DMSO) δ 172.68, 171.53, 155.63, 143.74, 143.66, 140.60, 138.06, 137.31, 129.18, 129.10, 128.13, 127.96, 127.57, 127.00, 126.39, 126.16, 125.29, 125.20, 120.01, 65.62, 64.86, 55.91, 53.41, 46.52, 37.37, 36.67.

HRMS (ESI-TOF, m/z) calculated for $C_{33}H_{30}N_2O_5$ $[M + Na]^+$ 557.57, found 557.2035 (Appendix 2).

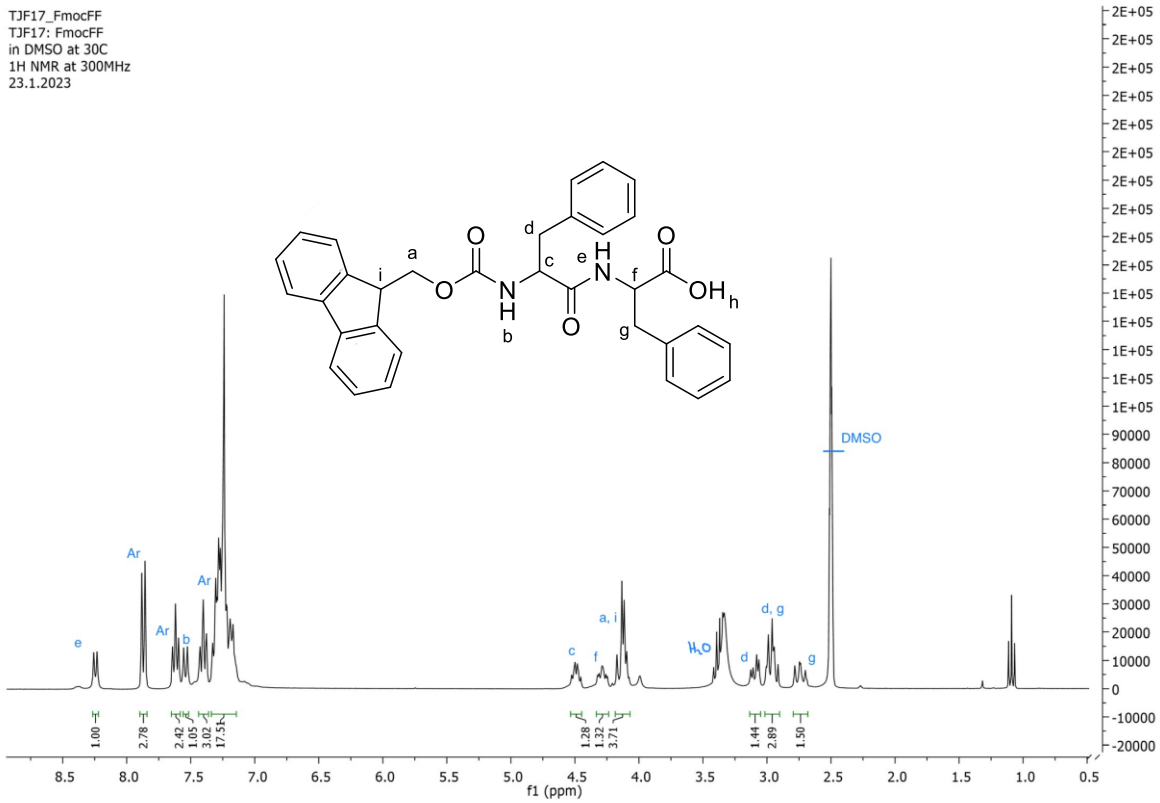

Figure 15. ^{1}H NMR (300 MHz, d_6-DMSO) spectrum of FmocFFCOOH.

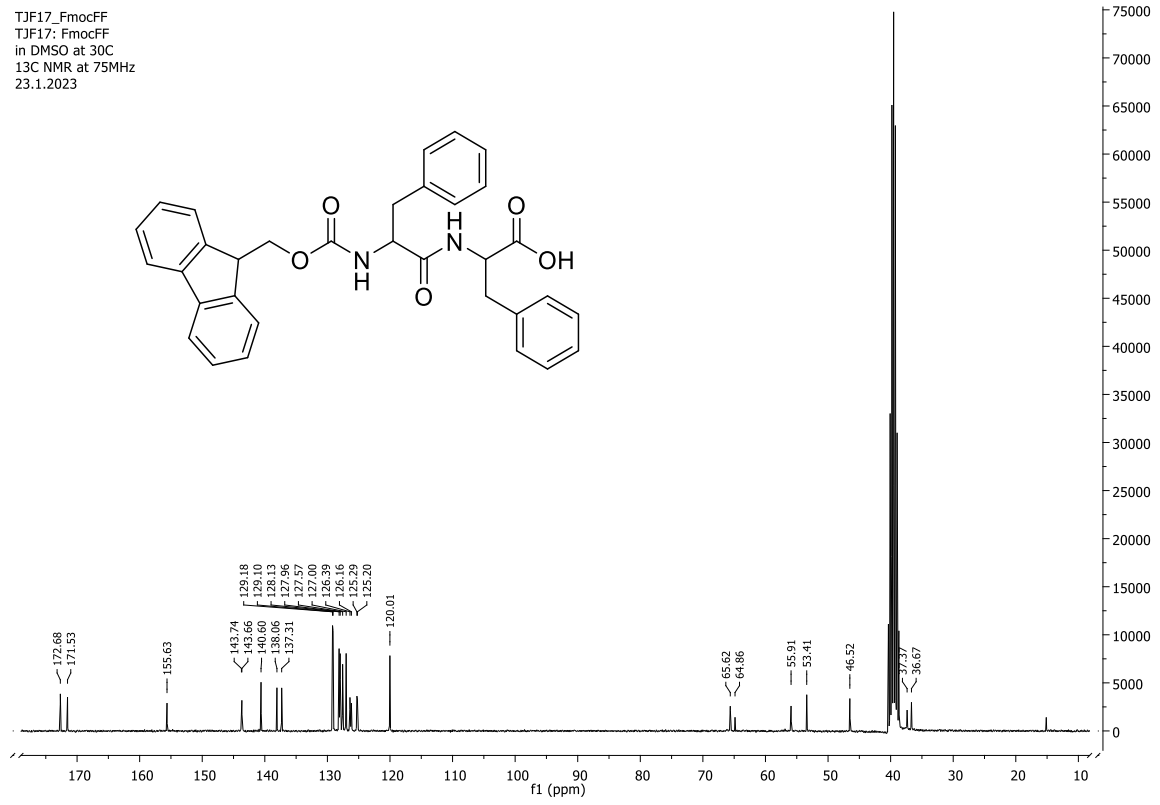

Figure 16. ^{13}C NMR (75 MHz, d_6-DMSO) spectrum of FmocFFCOOH.

9.2 Synthetic protocols for CinFFCOOH 2

9.2.1 Synthesis of BocFFO*t*Bu 4

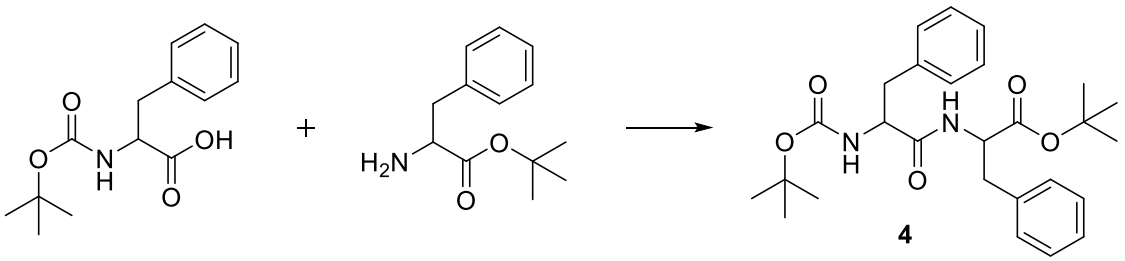

Scheme 11. The coupling reaction for the synthesis of BocFFO*t*Bu **4**.

BocF (1.13g, 1.0 eq), TBTU (1.21g, 1.0 eq), FOtBu (1.07g, 1.1 eq) and $NaHCO_3$ (0.66g, 1.1 eq) were dissolved in DMF (20 mL) under N_2 atmosphere. The solution was left to stir overnight at RT. The next day TLC (Hex:EA = 1:1, Hanessian´s stain) verified the consumption of the starting materials and the formation of the desired product (R_f = 0.57). The solvent was evaporated under vacuum by co-evaporation with toluene 3 times and the residue was dissolved in DCM. The organic phase was extracted with water (x2) and washed with aq. HCl (0.1 M) (x2), water (x2) and then with saturated aq. solution of $NaHCO_3$. The organic phase was dried with $MgSO_4$, evaporated and dried under vacuum overnight yielding an off-yellow glassy solid powder (1.6815g, 84.1%).

The reaction was performed in four batches to obtain more material for further synthetic steps as they appeared to be problematic. Although all reactions were performed in identical manner, the obtained %-yields were different. The reasons for yield inconsistency is that some material was lost during the washings due to flask that was leaking or just not being precise enough. Also, the weighing might have been performed to “wet” product. The reaction codes and corresponding yields are listed below (Table 4).

Table 4. The yields of dipeptide BocFFO*t*Bu in different reaction batches. All four synthesis were performed under identical conditions.

Reaction code	Yield (g)	Yield (%)
TJF1	1.6815	84
TJF3	1.2881	64
TJF9	1.3259	67
TJF13	0.879	44

To prove the purity, we measured NMR and HR-MS spectra (from TJF1 sample). The ^{1}H (Figure 17) and ^{13}C (Figure 18) NMR spectra of BocFFO*t*Bu agree with previously published data.[2] The corresponding functional groups/moieties are highlighted in bolt letters in all ^{1}H NMR chemical shifts.

^{1}H NMR (300 MHz, DMSO) δ 8.19 (d, *J* = 7.2 Hz, 1H, N**H**), 7.34 – 7.16 (m, 10H, **Ar**), 6.83 (d, *J* = 8.7 Hz, 1H, N**H**), 4.43 – 4.33 (m, 1H, C**H**), 4.19 (s, 1H, C**H**), 3.01 – 2.93 (m, 2H, C**H**$_2$), 2.90 (d, *J* = 3.8 Hz, 2H, C**H**$_2$), 1.32 (s, 9H, ***t*Bu**), 1.29 (s, 9H, ***t*Bu**).

^{13}C NMR (126 MHz, DMSO) δ 171.76, 170.42, 155.17, 138.15, 137.10, 129.28, 129.17, 128.18, 127.99, 126.52, 126.17, 80.69, 77.97, 55.52, 54.11, 37.44, 36.88, 28.12, 27.50.

HRMS (ESI-TOF, m/z) calculated for $C_{27}H_{37}N_2O_5$ $[M + H]^+$ 469.27, found 469.2765. (Appendix 3)

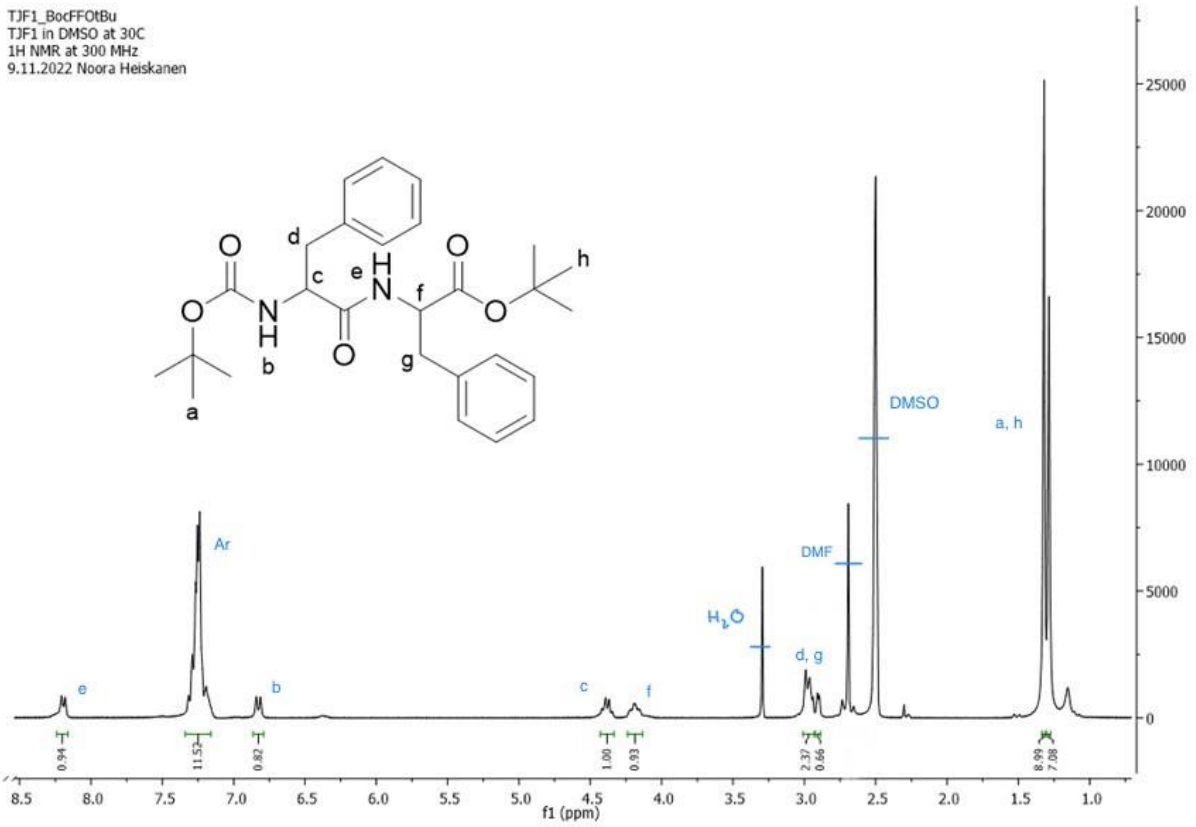

Figure 17. ^{1}H NMR (300 MHz, d_6-DMSO) spectrum of BocFFO*t*Bu.

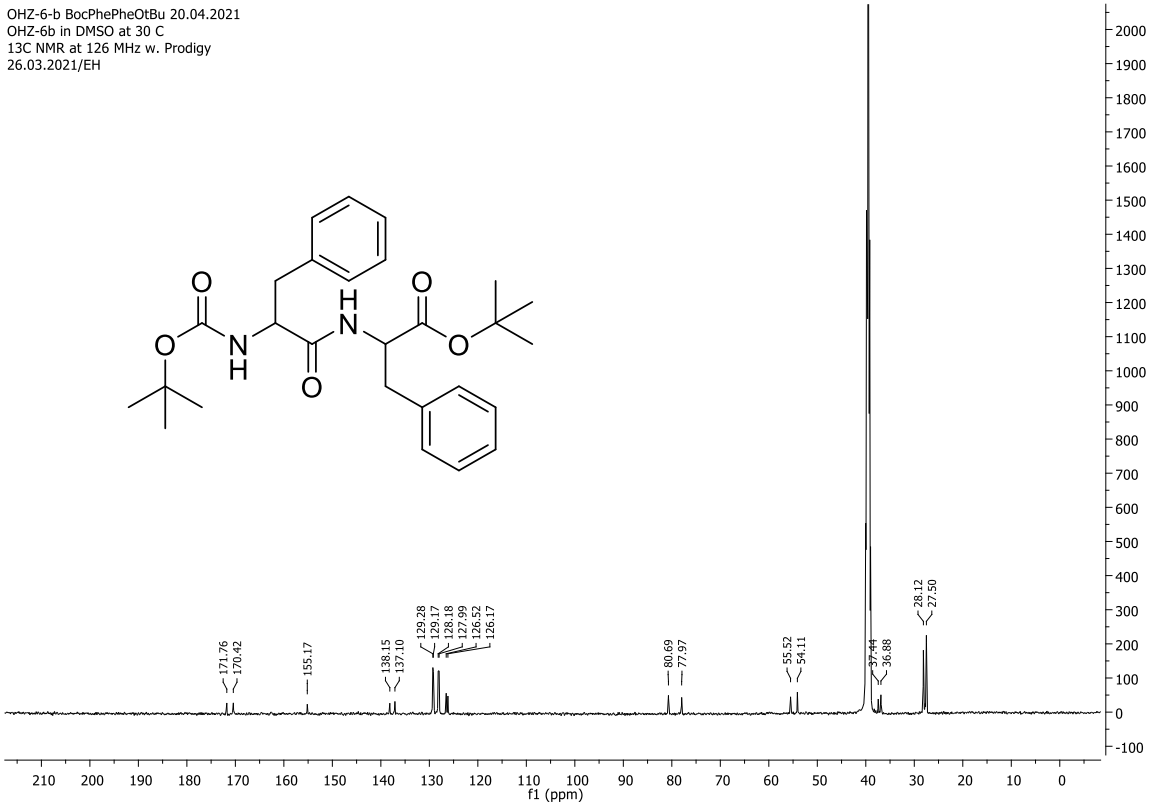

Figure 18. ^{13}C NMR (126 MHz, d_6-DMSO) spectrum of BocFFO*t*Bu.

9.2.2 Synthesis of FFO*t*Bu 5

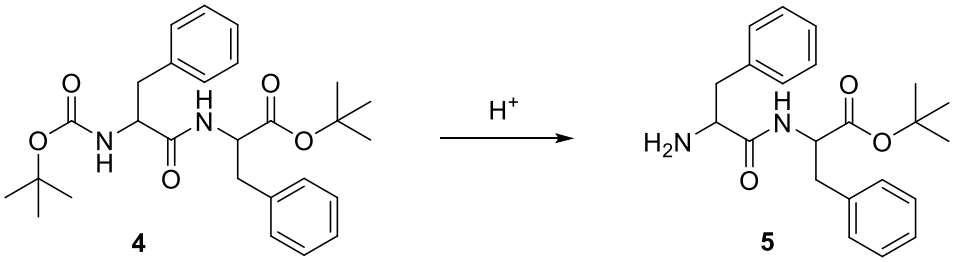

Scheme 12. Selective deprotection reaction of BocFFO*t*Bu **4** towards FFO*t*Bu **5**.

BocFFO*t*Bu **4** (0.832 g, 1.0 eq) was suspended in *tert*-butyl acetate (8.2 mL) at a final concentration of 0.2 M. Concentrated H_2SO_4 (0.472 mL, 5.0 eq) was added to the solution dropwise at RT, and the pH was measured (pH = 1-2). After 1h, TLC (Hex:EA, 3:1, Hanessian´s stain) confirmed that the reaction was completed. The reaction mixture was left to stir overnight and the next day, EA was added following the neutralization of the system (pH 7) by adding saturated aq. $NaHCO_3$. Extractions were followed with saturated aq. $NaHCO_3$ (x4) and then water (x2). The aquatic phase was back extracted with EA. The organic phases were combined and dried with $MgSO_4$ and evaporated to dryness. The obtained residue was left under vacuum overnight, giving an off-white solid in a stoichiometric yield 0.3856g.

The reaction was performed in five batches to optimize the reaction´s conditions and obtain more material for the following steps. The reaction codes and their yields are listed in Table 5.

Table 5. The yields of FFO*t*Bu at different reaction batches

Reaction code	Starting material (g)	Yield (stoichiometric-g)	Changes in procedure
TJF4	0.500	0.118	Primary no extractions were done. After one NMR it was decided to do $NaHCO_3$ and water (x2) washings
TJF6	0.743	0.631	No extractions were done
TJF11	0.832	0.386	Performed as described in synthesis
TJF14	0.458	0.578	Performed as described in synthesis
TJF15	0.879	0.365	Performed as described in synthesis

To prove the purity, we measured NMR and HR-MS spectra (from TJF4 sample). The ^{1}H (Figure 19) and ^{13}C (Figure 20) NMR spectra of FFO*t*Bu agree with previously published data.[2] The corresponding functional groups/moieties are highlighted in bolt letters in all ^{1}H NMR chemical shifts.

^{1}H NMR (300 MHz, DMSO) δ 8.15 (d, *J* = 7.6 Hz, 1H, N**H**$_2$), 7.30 – 7.12 (m, 11H, **Ar,** N**H**), 4.43 (q, *J* = 7.0 Hz, 1H, C**H**), 3.41 (dd, *J* = 8.2, 4.5 Hz, 2H, C**H**$_2$), 2.94 (d, *J* = 7.0 Hz, 2H, C**H**$_2$), 2.89 (d, *J* = 4.6 Hz, 1H, C**H**$_2$), 2.57 (d, *J* = 5.0 Hz, 1H, C**H**$_2$), 1.33 (s, 9H, **O*t*Bu**).

^{13}C NMR (126 MHz, DMSO) δ 174.07, 170.42, 138.56, 136.90, 129.36, 129.26, 128.14, 128.07, 126.53, 126.10, 80.85, 55.77, 53.43, 40.71, 37.21, 27.52.

HR-MS (ESI-TOF, m/z) calculated for $C_{22}H_{29}N_2O_3$ $[M + H]^+$ 369.21, found 369.2161. (Appendix 4)

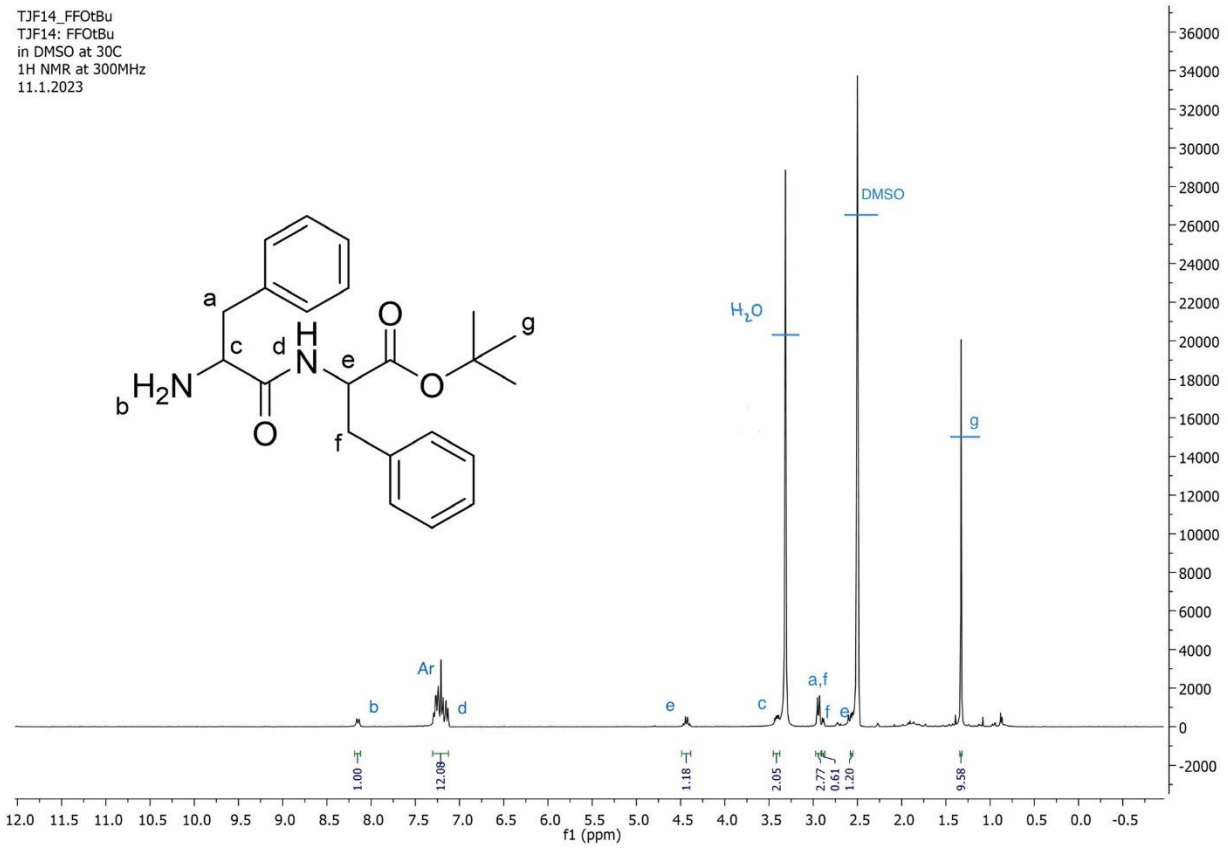

Figure 19. ^{1}H NMR (300 MHz, d_6-DMSO) spectrum of FFO*t*Bu.

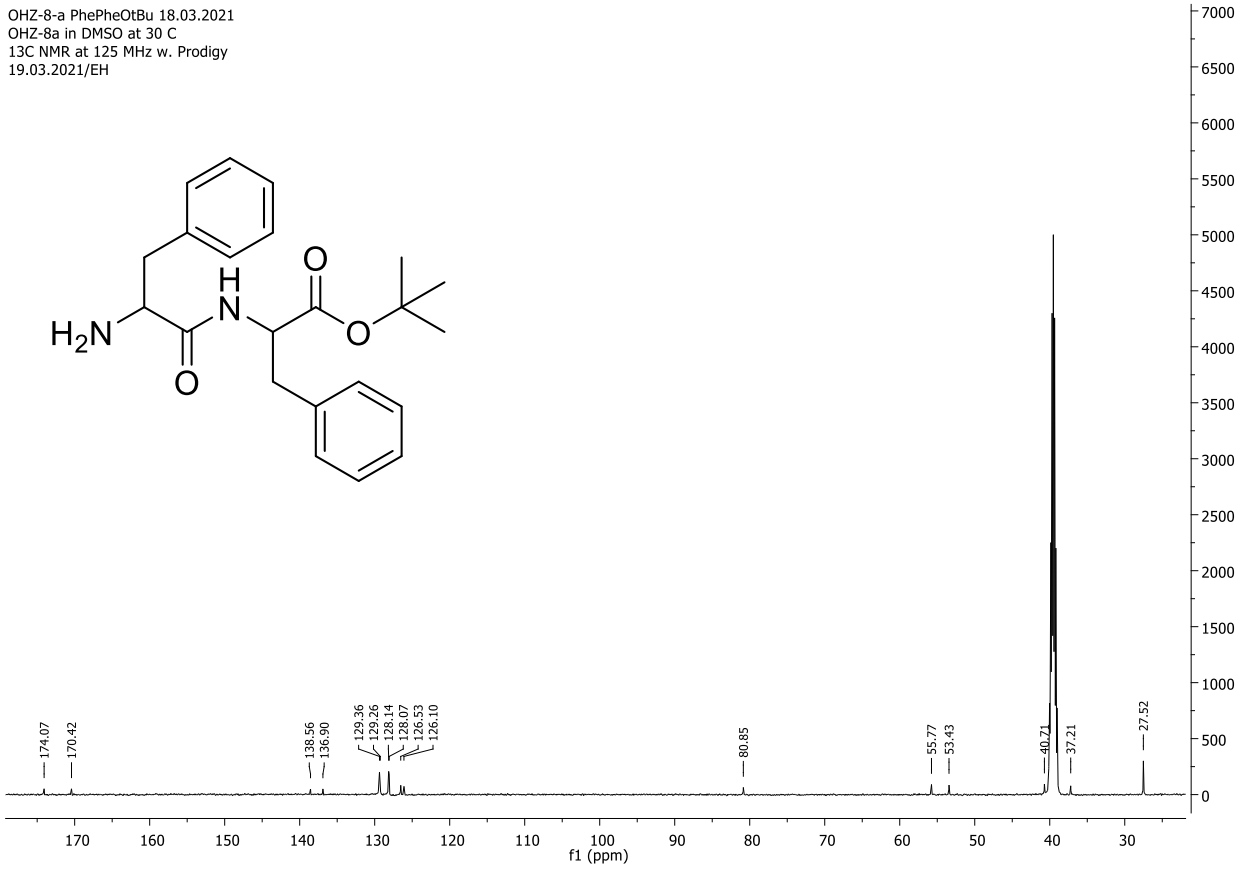

Figure 20. ^{13}C NMR (126 MHz, d_6-DMSO) spectrum of FFO*t*Bu.

9.2.3 Synthesis of CinFFO*t*Bu 6

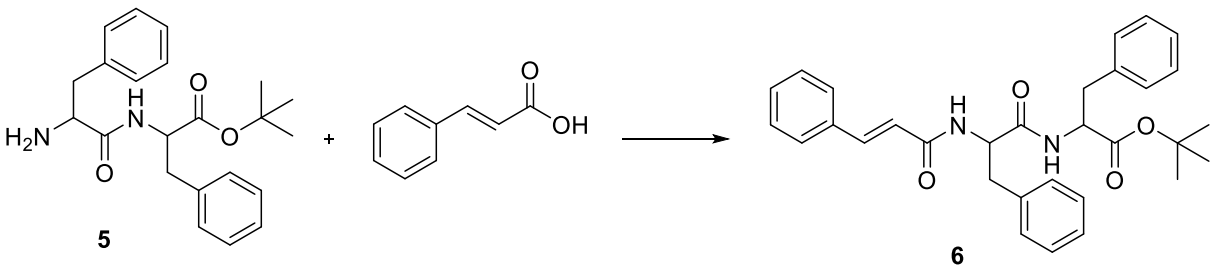

Scheme 13. The addition of the cinnamoyl group to FFO*t*Bu **5** to produce CinFFO*t*Bu **6**.

Cinnamic acid (57 mg, 1.2eq), $NaHCO_3$ (67 mg, 2.5eq) and TBTU (154 mg, 1.5eq) were added to anhydrous DMF (1 mL) under the N_2 atmosphere. The solution was left to stir for 30 min at RT before the addition of FFO*t*Bu **5** dipeptide (118 mg, 1.0 eq). The reaction was left to stir overnight under the same conditions.

The next day, TLC (Hex:EA = 1:1, Hanessian's stain) showed that the reaction was finished. The solvent was then evaporated, and the residue was dissolved in EA (10 mL) and extracted with water (x3). The organic phase was dried with $MgSO_4$ and evaporated to dryness.

The obtained residue was purified with flash column chromatography. The solvent systems usedwere 150 mL 4:1, Hex:EA and 3:1, Hex:EA (in total 1L). Fractions 25-54 were named mixture B. The mixture B was partially evaporated and filtrated. Then the mixture was placed under a vacuum to evaporate the remaining solvent. The obtained residue was further dissolved in methanol, filtrated, and dried under a vacuum. The product (0.0198 g) was obtained at a yield of 12%.

The reaction was conducted three times to obtain more material for last synthetic step. All three batches were performed under identical conditions. The corresponding yields are given in Table 6.

Table 6. Reaction batches and corresponding yields of the CinFFO*t*Bu preparation.

Reaction code	Starting material (g)	Yield (g)	Yield (%)
TJF7	0.118	0.0198	12
TJF8	0.631	0.1056	12
TJF12 + TJF16	0.385 + 0.578	0.3078	24

To prove the purity, we measured NMR and HR-MS spectra (from TJF7 sample). The ^{1}H (Figure 21) and ^{13}C (Figure 22) NMR spectra of CinFFO*t*Bu agree with previously published data.[2] The corresponding functional groups/moieties are highlighted in bolt letters in all ^{1}H NMR chemical shifts.

^{1}H NMR (400 MHz, DMSO) δ 8.50 (d, J = 7.3 Hz, 1H, N**H**), 8.32 (d, J = 8.7 Hz, 1H, N**H**), 7.53 (m, J = 6.7 Hz, 2H, **Ar**), 7.40 (dd, J = 12.3, 4.7 Hz, 3H, **Ar**), 7.37 – 7.35 (m, 1H, C**H**), 7.23 (m, 10H, **Ar**), 6.67 (d, J = 15.8 Hz, 1H, C**H**), 4.72 (td, J = 9.9, 3.9 Hz, 1H, C**H**), 4.38 (q, J = 7.3 Hz, 1H, C**H**), 3.06 (dd, J = 13.9, 3.9 Hz, 1H, C**H**$_2$), 3.01 – 2.93 (m, 2H, C**H**$_2$), 2.78 (dd, J = 13.8, 10.3 Hz, 1H, C**H**$_2$), 1.32 (s, 9H, ***t*Bu**).

^{13}C NMR (100 MHz, DMSO) δ 171.13, 170.19, 164.61, 138.87, 137.74, 137.00, 134.76, 129.34, 129.10, 129.04, 128.81, 128.05, 127.90, 127.39, 126.37, 126.14, 121.85, 80.60, 54.13, 53.55, 37.59, 36.78, 27.44.

HR-MS (ESI-TOF, m/z) calculated for $C_{31}H_{34}N_2O_4$ $[M + Na]^+$ 521.24, found 521.2419. (Appendix 5)

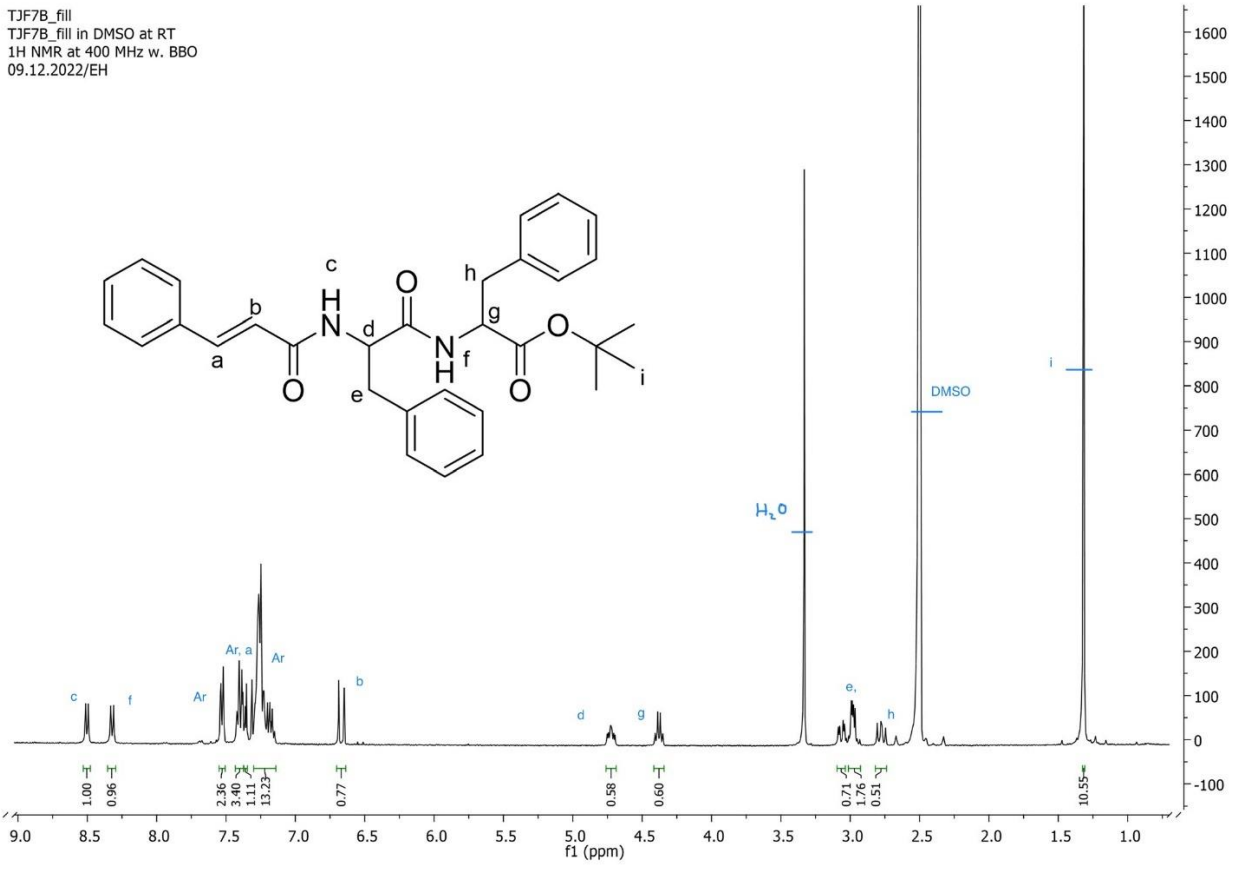

Figure 21. ^{1}H NMR (300 MHz, d_6-DMSO) spectrum of CinFFO*t*Bu.

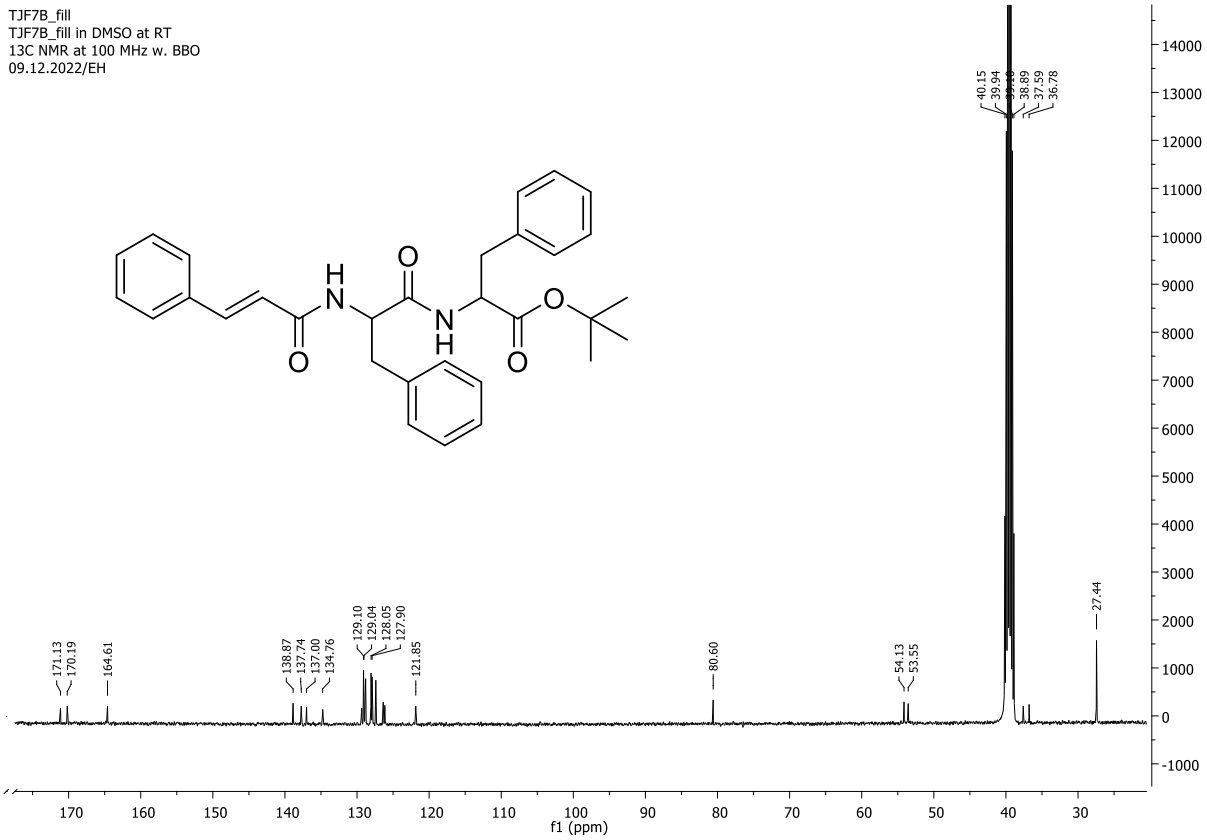

Figure 22. ^{13}C NMR (100 MHz, d_6-DMSO) spectrum of CinFFO*t*Bu.

9.2.4 Synthesis of CinFFCOOH 2

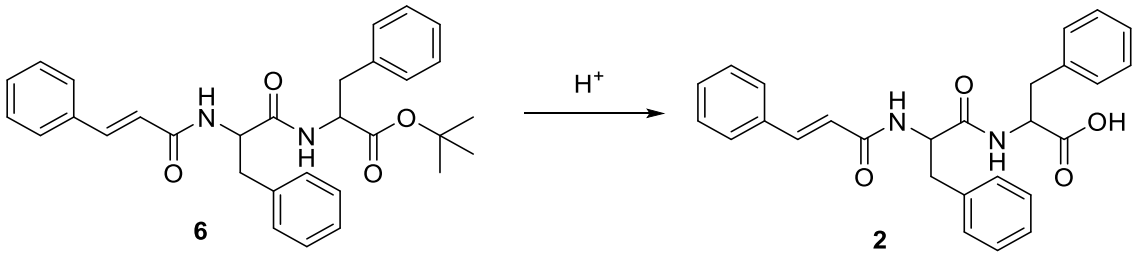

Scheme 14. Selective deprotection reaction of CinFFO*t*Bu **6** towards CinFFCOOH **2**.

CinFFO*t*Bu **6** (0.3073 g, 1.0eq) was dissolved in DCM (1.5 mL) followed by the addition of TFA (0.92 mL) at 0°C dropwise. The reaction was left to stir for 3-4 hours in RT. TLC (Hex:EA, 1:1, Hanessian's stain) showed that the reaction was incomplete. Therefore, extra TFA (0.92 mL) was added. After an hour TLC (Hex:EA, 1:1, Hanessian's stain) confirmed the completion of the reaction. The solvent was co-evaporated three times with DCM to dryness giving an off-yellow solid which was dried overnight under vacuum. The product was obtained at stoichiometric yield (0.241 g).

The reaction was conducted two times as the first batch was too small to proceed with gelation experiments. The corresponding yields are given in Table 7.

Table 7. Deprotection reactions and corresponding yields of CinFFCOOH

Reaction code	Starting material (g)	Yield (stoichiometric-g)
TJF10	0.020	~ 0.010
TJF19	0.3073	0.241

To prove the purity, we measured NMR spectra (from TJF10 sample). The ^{1}H (Figure 23) and ^{13}C (Figure 24) NMR spectra of CinFFCOOH agree with previously published data.[2] The corresponding functional groups/moieties are highlighted in bolt letters in all ^{1}H NMR chemical shifts. NMR spectra measured from sample TJF19 included some impurities, unlike this spectrum measured with TJF10.

^{1}H NMR (300 MHz, DMSO) δ 8.35 (d, *J* = 7.8 Hz, 1H, N**H**), 8.26 (d, *J* = 8.5 Hz, 1H, N**H**), 7.53 (dd, *J* = 7.8, 1.4 Hz, 2H, **Ar**), 7.41 (dd, *J* = 11.1, 5.2 Hz, 3H, **Ar**), 7.36 (d, J = 4.3 Hz, 1H, C**H**), 7.33 – 7.12 (m, 10H, **Ar**), 6.67 (d, *J* = 15.8 Hz, 1H, C**H**), 4.71 (td, *J* = 9.7, 4.1 Hz, 1H, C**H**), 4.48 (td, *J* = 8.3, 5.3 Hz, 1H, C**H**), 3.08 (ddd, *J* = 14.5, 10.2, 4.7 Hz, 2H, C**H$_2$**), 2.95 (dd, *J* = 13.9, 8.7 Hz, 1H, C**H**$_2$), 2.77 (dd, *J* = 14.0, 10.1 Hz, 1H, C**H$_2$**).

^{13}C NMR (75 MHz, DMSO) δ 172.66, 171.26, 164.68, 138.98, 137.86, 137.39, 134.84, 129.45, 129.14, 128.91, 128.17, 128.00, 127.50, 126.40, 126.21, 121.90, 53.69, 53.46, 37.56, 36.67.

HR-MS not done due to the lack of compound and observed impurities in the NMR spectra measured from sample TJF19.

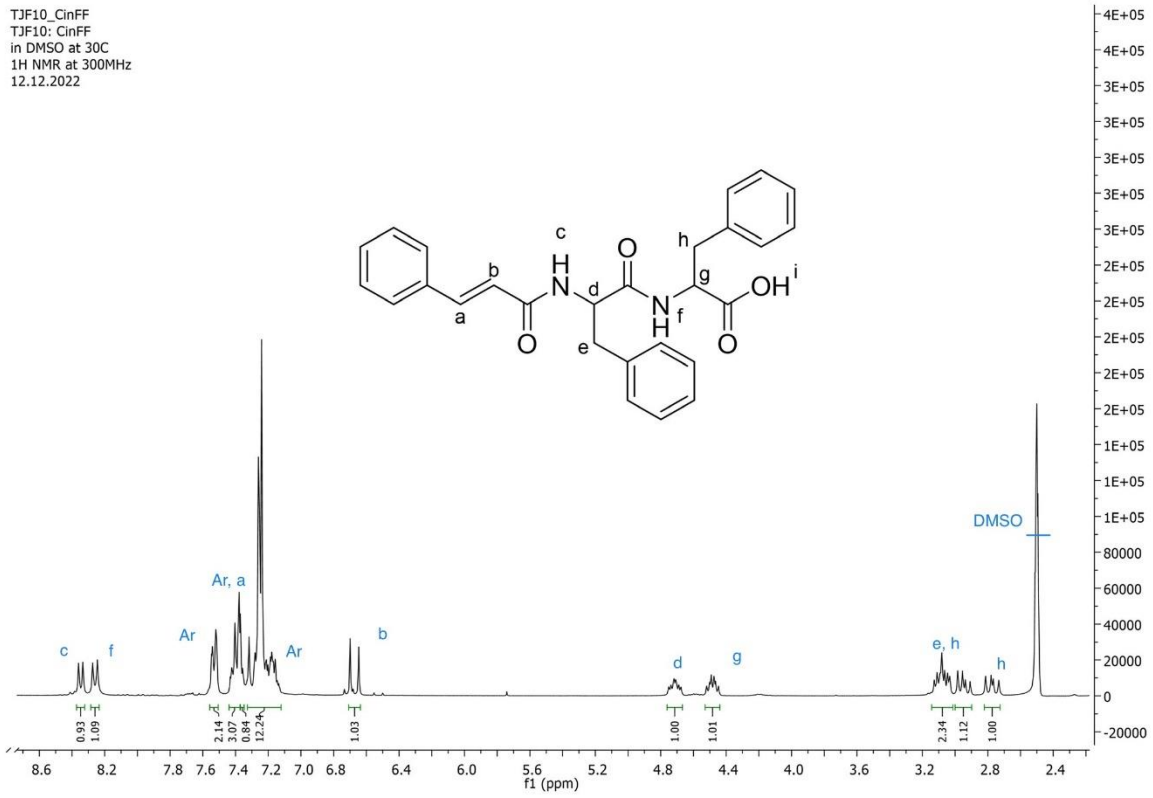

Figure 23. ^{1}H NMR (300 MHz, d_6-DMSO) spectrum of CinFFCOOH.

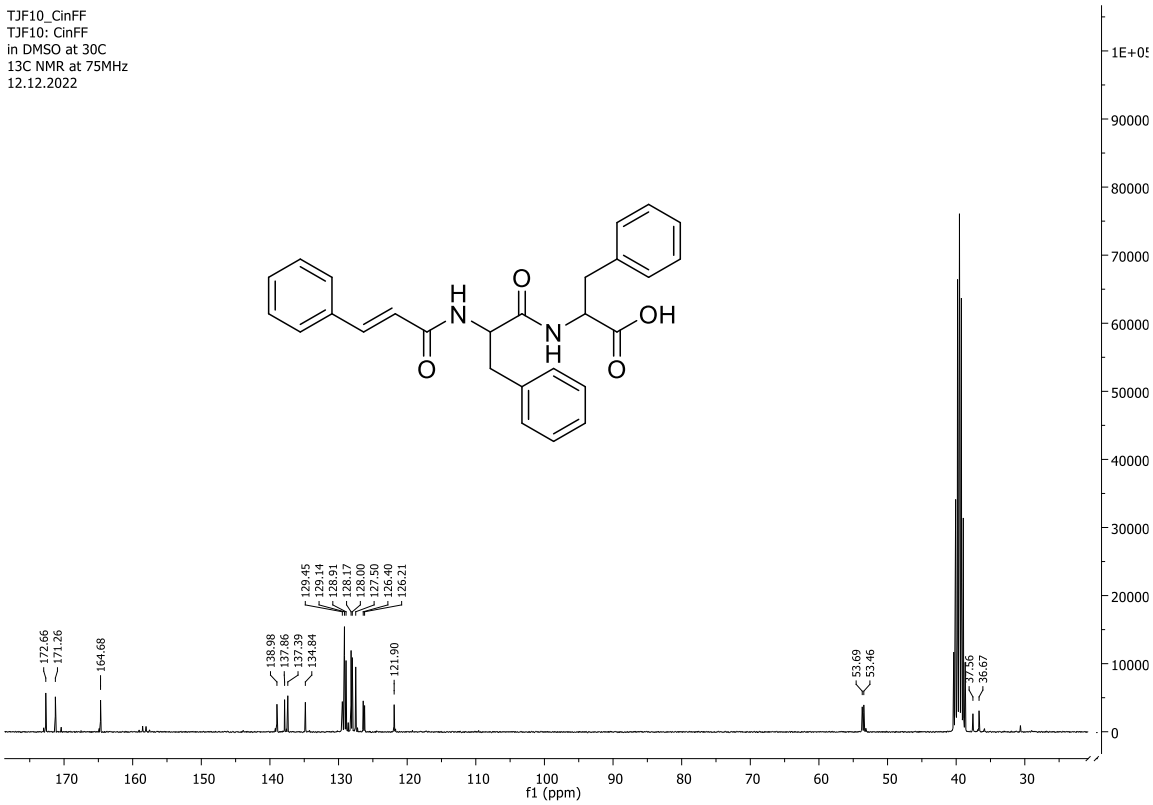

Figure 24. ^{13}C NMR (75 MHz, d_6-DMSO) spectrum of CinFFCOOH.

10 Gelation trials of FmocFFCOOH

Gels were prepared in different ways to find the optimal gelation conditions. Firstly, with sample A, the pH was changed. FmocFFCOOH (2.0 mg) was diluted in PBS solution (1.0 mL, 50 mM) and sonicated until dissolved. Afterwards aq. solution of KOH (10 µL, 1.0 M) was added, and the gelation occurred. A second sample (sample B) was prepared following the protocol of sample A, but the PBS solution was different (ready-made solution; Fisher BioReagents, NaCl 137mM, phosphate buffer 10mM, KCl 2.7mM, pH 7.4, one tablet dissolved in /100mL of deionized H_2O).

In sample C, FmocFFCOOH (2.0 mg) was suspended in 1.0 mL of deionized H_2O and sonicated until completely dissolved. Aq. solution of KOH (10 µl, 1.0 M) was initially added followed by the addition of HCl solution (10 µl, 1.0 M). It is of note that none of the samples A-C gelled rapidly. Therefore, they were left undisturbed overnight for gelation to occur.

In addition, we tried the heating and cooling method to induce gelation. In sample D, FmocFFCOOH (2.0 mg) was dissolved in 1.0 mL PBS and heated for 30 minutes at 80°C. In sample E, 5.0 mg of FmocFFCOOH was used following the same protocol as sample D.

Gelation was also assessed by the solvent exchange method. In sample F, FmocFFCOOH (2.0 mg) was dissolved in 50 µL of DMSO while 950 µL of PBS was added afterwards. The same protocol was followed for sample G, but the concentration of FmocFFCOOH increased to 5.0 mg/mL.

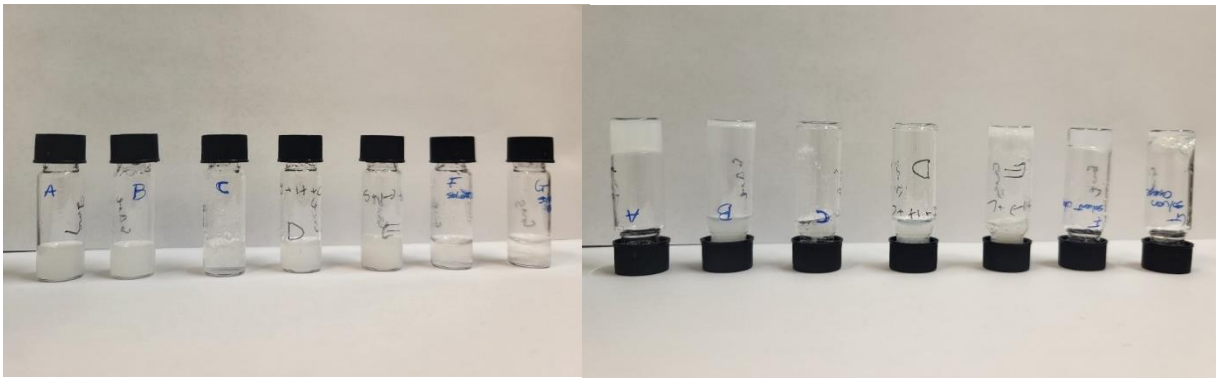

Figure 25. The vial inversion test of samples A-G on day 1.

Based on the vial inversion test (Figure 25), sample A yielded a self-supporting hydrogel while samples E,F and G were partially gelled. All results are presented in Table 8. By the vial inversion test we observed the free gravitational flow of yhe gelling material.

Table 8. The first set of gelation trials

	Concentration (mg/mL)	**Gelation method**	**Solvent**	**Result**
A	2.0	pH change	PBS	Self-supporting gel*
B	2.0	pH change	PBS	No stable long-term gelation
C	2.0	pH change	H_2O	No stable long-term gelation
D	2.0	Heating and cooling	PBS	No gelation
E	5.0	Heating and cooling	PBS	Partial gelation
F	2.0	Solvent exchange	PBS	Partial gelation
G	5.0	Solvent exchange	PBS	Partial gelation

‘ Only protocol A yielded a self-supporting gel.

The next phase of the gelation studies refer to the reproducibility of the gelation procedure. Therefore, the gel samples were prepared in triplicate following the same protocols as above. More specifically gelation trials were performed as follows:

- Samples A-C: 2.0 mg of FmocFFCOOH were dissolved in 1.0 mL of PBS, sonicated and left undisturbed overnight.
- Samples D-F: 2.0 mg of FmocFFCOOH were dissolved in 1.0 mL of PBS sonicated and heated for 30 min at 80°C.

Figure 26 reveals that gelation occurred in all samples, however for A-C samples gelation was more effective; robust gels were produced which passed the vial inversion test.

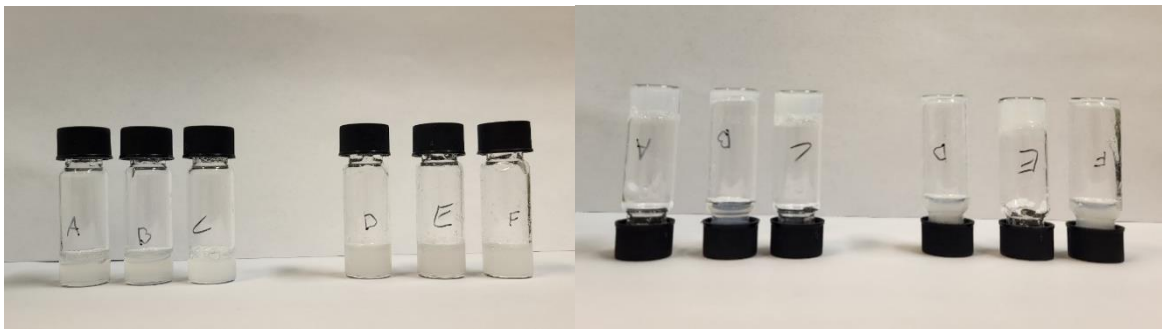

Figure 26. The vial inversion test for samples A-C and D-F on day 1.

In addition, a stock solution of FmocFFCOOH was prepared by diluting 200mg of FmocFFCOOH in 1.0 mL of DMSO. This solution was used to prepare the following samples:

- Samples G-I: 10 µL of the stock solution were transferred in a vial and 990 µL of PBS solution was added.
- Samples J-L: 990 µL PBS solution were added in a vial, and 10 µL of the stock solution was added afterwards.
- Samples M-O: 10 µL of the stock solution was added in a vial and 990 µL of deionized water was added afterwards.
- Samples P-R: 990 µL of deionized water was added in a vial followed by 10 µL of the stock solution.

All samples (Figure 27) were only slightly swirled as to mix the two solutions as gelation occurred immediately after adding the second solvent.

Figure 27. The vial inversion test of samples G-I, J-L, M-O and P-R at day 1.

The gelation trial using PBS and following the solvent exchange method was not effective. Only for samples G-I partial gelation was observed at the DMSO face, but the gel was not homogeneous. In contrast, gelation trials yielded better reproducible results when water was used.

All the above samples (G-R) were reheated for 30 minutes at 80°C and left to cool down overnight to assess if heating induced the solubilization and potential gelation of FmocFFCOOH. Homogeneous gels formed (the results are presented in Figures 28 and 29). Reheating was not effective as some of the gels broke. Only sample I formed a self-supporting gel meaning that heating was more effective compared to the initial solvent exchange trial (see above).

Figure 28. The vial inversion test of samples G-I and J-L after heating and cooling (day 1).

Figure 29. The vial inversion test of samples Q and M demonstrates that the gelation ability of the samples is not altered after re heating and cooling (thermoreversible gels).

All the results for samples A-R in this second trial are presented in Table 9.

Table 9. The second set of gelation trials

	Concentration (mg/mL)	**Gelation method**	**Solvent**	**Result**
A-C	2.0	Sonication	PBS	Gelation
D-F	2.0	Heating and cooling	PBS	Gelation in sample E
G-I	2.0	Solvent exchange	PBS/DMSO	Partial gelation
J-L	2.0	Solvent exchange	PBS/DMSO	Partial gelation
M-O	2.0	Solvent exchange	PBS/DMSO	Partial gelation
P-R	2.0	Solvent exchange	PBS/DMSO	Partial gelation

Gelation trials demonstrated the gelation ability of FmocFFCOOH as expected. Depending on the chosen gelation triggers the gelation outcome was different. The best results were received for samples A-C (2.0 mg/mL of FmocFFCOOH in PBS), as they formed clear gels, in a reproducible manner.

11 FTIR Spectroscopy results

FT-IR spectra were recorded for all compounds. The results and corresponding spectra are given below (Figures 30-34).

For FmocFFO*t*Bu **3** the most important functional groups can be seen in amide A region (3313 cm^{-1}), the aromatic C-H stretching region from 3062-2934 cm^{-1}, C=O group at 1732-1650 cm^{-1}, C=C bonds of aromatic ring at 1528-1450 cm^{-1}, C-N stretching at 1249 cm^{-1} and sharp peaks at 738 cm^{-1} and 698 cm^{-1} corresponding to N-H bonds (Figure 30).

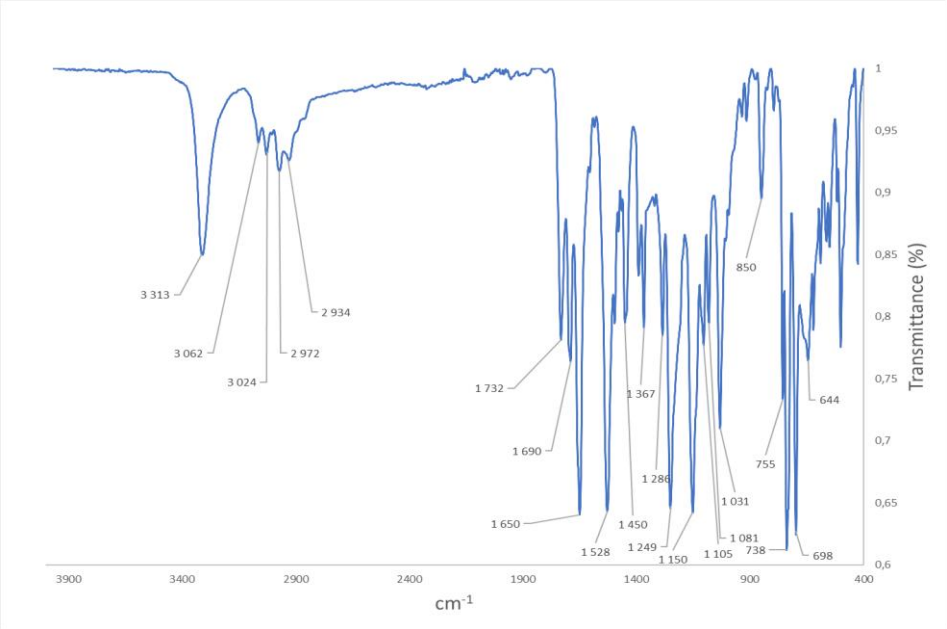

Figure 30. FT-IR spectrum of FmocFFO*t*Bu **3**; IR (v_{max}/ cm^{-1}): 3313 (s), 3062 (vw), 3024 (vw), 2972 (w), 2934 (wv), 1732 (s), 1690 (s), 1650 (s), 1528 (s), 1450 (w), 1367 (w), 1286 (w), 1249 (s), 1150 (s), 1105 (w), 1081 (w), 1031 (s), 850 (w), 755 (w), 738 (s), 698 (s), 644 (w) cm^{-1}.

For FmocFFCOOH **1** the most important functional groups can be seen in the amide A region (3292 cm^{-1}), the aromatic C-H stretching is seen around 3027 cm^{-1} and 2955 cm^{-1}, C=O group is seen in 1693-1652 cm^{-1}, 1530-1496 cm^{-1} shows CH=CH bonds of aromatic ring, 1249 cm^{-1} is from C-N stretching and sharp peaks at 737 cm^{-1} and 698 cm^{-1} corresponds to N-H bonds (Figure 31).

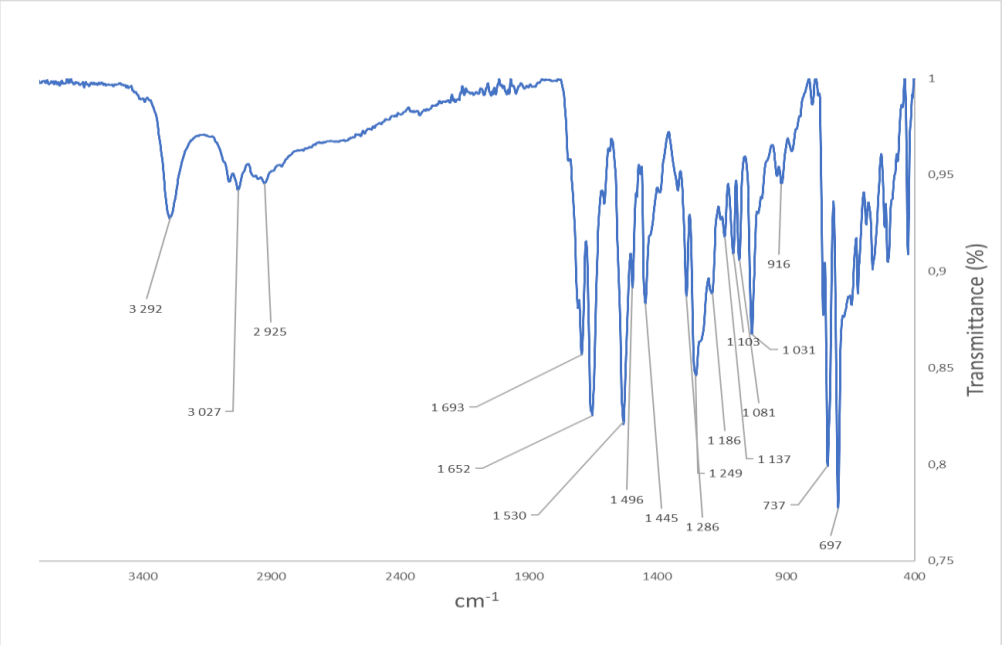

Figure 31. FT-IR spectrum of FmocFFCOOH **1**; IR (v_{max}/ cm^{-1}): 3292 (br), 3027 (vw), 2925 (vw), 1693 (s), 1652 (s), 1530 (s), 1496 (sh), 1445 (s), 1286 (w), 1249 (s), 1186 (sh), 1137 (w), 1103 (w), 1081 (w), 1031 (s), 916 (w), 737 (s), 697 (s) cm^{-1}.

For BocFFO*t*Bu **4** the most important functional groups can be seen in amide A region (3293 cm^{-1}), the aromatic C-H stretching is seen in 2977-2935 cm^{-1} and, C=O group is seen in 1731-1652 cm^{-1}, 1518-1455 cm^{-1} shows CH=CH bonds of aromatic ring, 1152 cm^{-1} is from C-N stretching and 698 cm^{-1} corresponds to N-H bonds (Figure 32).

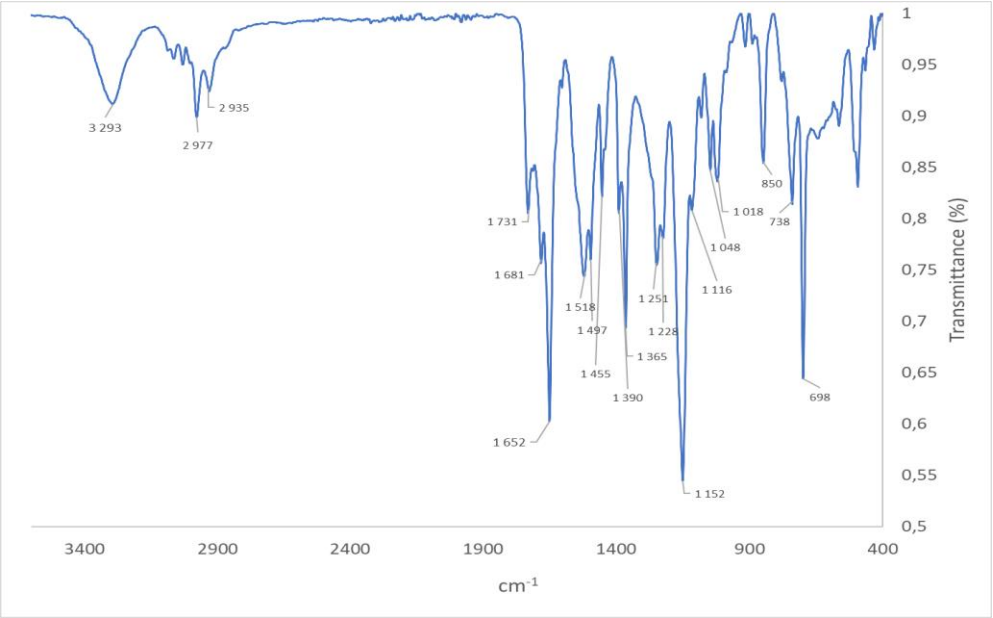

Figure 32. FT-IR spectrum of BocFFO*t*Bu **4**; IR (v_{max}/ cm^{-1}): 3293 (br), 2977 (w), 2935, (vw), 1731 (sh), 1681 (sh), 1652 (s), 1518 (s), 1497 (m), 1455 (w), 1390 (sh), 1365 (s), 1251 (s), 1228 (sh), 1152 (s), 1116 (sh), 1048 (w), 1018 (w), 850 (s), 738 (s), 698 (s) cm^{-1}.

For FFO*t*Bu **5** the most important functional groups can be seen in the amide A region (3332 cm^{-1}), the aromatic C-H stretching is seen around 2979 cm^{-1} and the C=O group is seen in 1711 cm^{-1}, 1528-1497 cm^{-1} shows CH=CH bonds of aromatic ring, 1154 cm^{-1} is from C-N stretching and two strong peaks at 742 cm^{-1} and 700 cm^{-1} corresponds to N-H and NH_2 bonds (Figure 33).

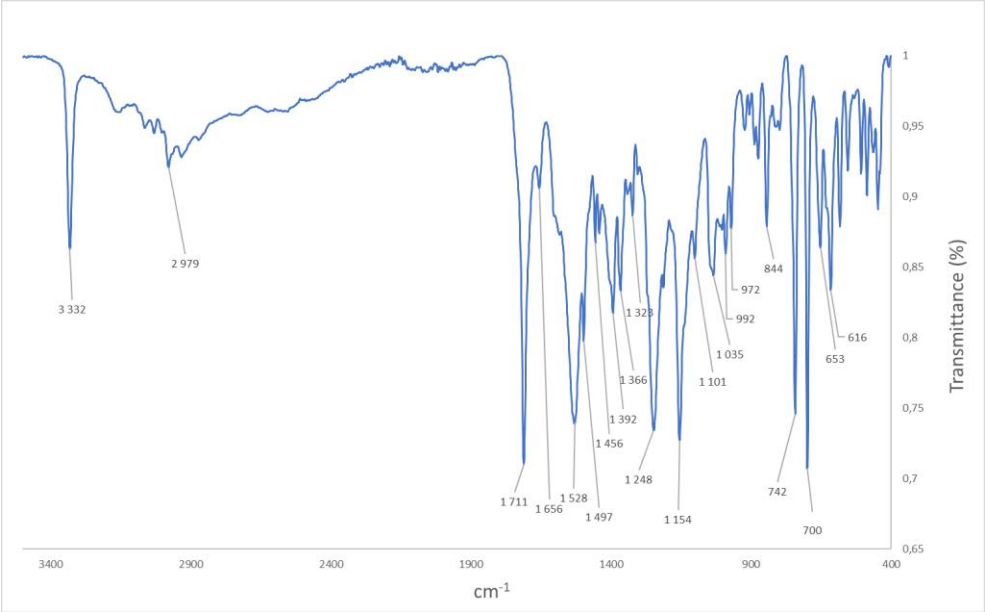

Figure 33. FT-IR spectrum of FFO*t*Bu **5**; IR (vmax/ cm^{-1}): 3332 (s), 2979 (vw), 1711 (s), 1656 (sh), 1528 (s), 1497 (sh), 1456 (vw), 1392 (w), 1366 (w), 1323 (vw), 1248 (s), 1154 (s), 1101 (sh), 1035 (w), 992 (vw), 972 (vw), 844 (s), 742 (s), 700 (s), 653 (w), 616 (w) cm^{-1}.

For CinFFO*t*Bu **6** the most important functional groups can be seen in the amide A region (3299 cm^{-1}), the aromatic C-H stretching is seen from 3082-2931 cm^{-1}, C=O groups is seen in 1737 cm^{-1} and 1655-1626 cm^{-1}, 1538-1494 cm^{-1} shows CH=CH bonds of aromatic ring, 1156 cm^{-1} is from C-N stretching and the strong peak at 697 cm^{-1} corresponds to N-H bonds (Figure 34).

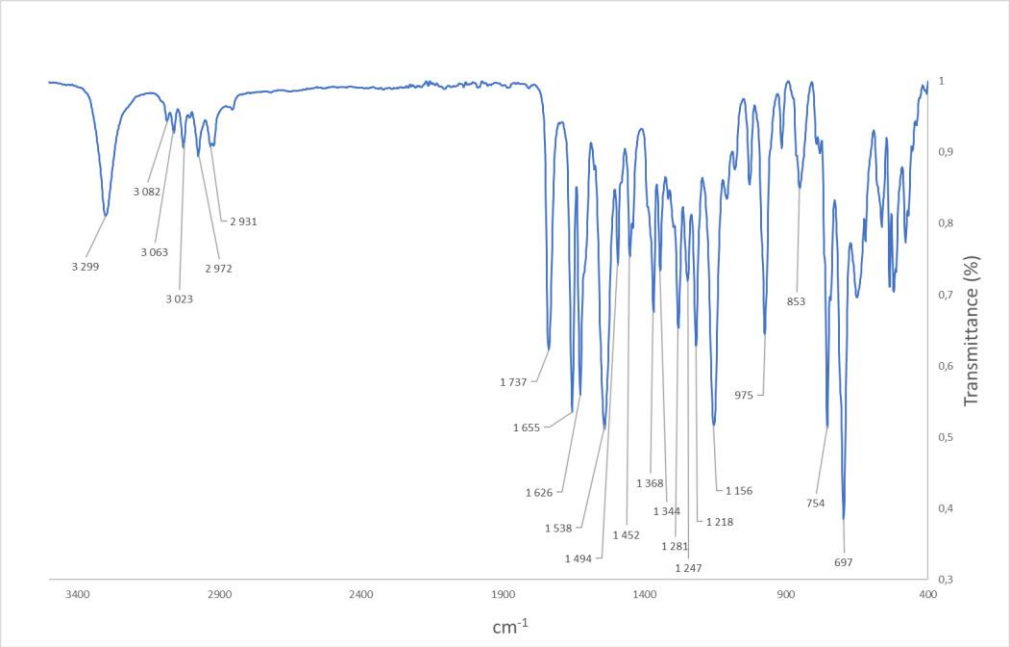

Figure 34. FT-IR spectrum of CinFFO*t*Bu **6**; IR (v_{max}/ cm^{-1}): 3299 (br), 3082 (vw), 3063 (vw), 3023 (vw), 2972 (vw), 2931 (w), 1737 (s), 1655 (s), 1626 (s), 1538 (s), 1494 (sh), 1452 (w), 1368 (w), 1344 (w), 1281 (s), 1247 (w), 1218 (s), 1156 (s), 975 (s), 853 (s), 754 (s), 697 (s) cm^{-1}.

For CinFFCOOH no FT-IR spectrum was recorded due to the lack of sufficient amount of the purified dipeptide.

12 Conclusions

The main goal of the research work was to synthesize the similar structurally dipeptides FmocFFCOOH and CinFFCOOH and compare their gelation behaviour. The spectroscopy assessment of the compounds by NMR, HR-MS and FT-IR proved that both compounds are possible to synthesise as pure compounds. However, some problems were observed during the syntheses. Yields turned out to be quite small for some batches and the second trial for CinFFCOOH didn´t result a pure product. Due to these reasons the gelation behaviour trials for the cinnamoyl derivative was not performed.

The conducted gelation experiments with FmocFFCOOH showed promising results, although not all gelation triggers were successful. It is of note that in some cases, while testing the gelation conditions in triplicate to assess reproducibility, the gelation outcome was not consistent. The best results were received with samples A-C (2.0 mg/mL of FmocFFCOOH in PBS by sonication method). These samples formed a self-supporting transparent gel; in triplicate.

The project may be continued by the gelation assessment of cinnamoyl dipeptide and comparison of the results to its corresponding Fmoc-protected counterpart. In addition, a revised protocol for the optimal synthesis and purification of the cinnamoyl dipeptide may be introduced. Indeed, the third step for the synthesis of CinFFCOOH was problematic. Therefore, different types of acids at different concentrations should be tested for the stoichiometric deprotection of the *tert*-butyl ester and the isolation of the pure compound. In addition, the reaction conditions during the second step gave low yields, while there were issues with the isolation of the intermediate CinFFCO*t*Bu by flash column chromatography. Finally, it would be interesting to assess the biocompatibility of the compounds at the solution and gel phases using different cell lines.

REFERENCES

1. Draper, E.R. and Adams D.J., Low-Molecular-Weight Gels: The State of the Art, *Chem*., **2017**, *3*, 390–410.
2. Sitsanidis, E.D., Kasapidou, P.M., Hiscock, J.R., Gubala, V., Castel, H., Popoola, P. I. A., Hall A. J. and Edwardset A. A., Probing the self-assembly and anti-glioblastoma efficacy of a cinnamoyl-capped dipeptide hydrogelator, *Org. Biomol. Chem.* **2022**, *20*, 7458–7466.
3. Shi, J., Gao, Y., Yang, Z., Xu, B., Exceptionally small supramolecular hydrogelators based on aromatic-aromatic interactions, *Beilstein J. Org. Chem.*, **2011**, *7*, 167–172.
4. De Loos, M., Feringa B.L., Van Esch, J.H., Design and application of self-assembled low molecular weight hydrogels, *Eur. J. Org. Chem*., **2005**, *17*, 3615–3631.
5. Ahmad, Z., Salman, S., Khan, S.A., Amin, A., Rahman, Z.U., Al-Ghamdi, Y.O., Akhtar, K., Bakhsh, E.M., Khan, S.B., Versatility of Hydrogels: From Synthetic Strategies, Classification, and Properties to Biomedical Applications, *Gels*, **2022**, *8*, 167.
6. Gyles, D.A., Castro, L.D., Silva J.O.C., Ribeiro-Costa, R.M., A review of the designs and prominent biomedical advances of natural and synthetic hydrogel formulations, *Eur. Pol. Jour.*, **2017**, *88*, 373–392.
7. Madduma-Bandarage, U.S.K. and Madihally, S. V., Synthetic hydrogels: Synthesis, novel trends, and applications, *Jour. of App. Pol. Sci*., **2020**, *138*, 50376.
8. Caliari, S.R. and Burdick, J.A., A practical guide to hydrogels for cell culture, *Nat. Meth*, **2016**, *13*, 405–414.
9. Sarrigiannidis, S.O., Rey, J.M., Dobre, O., Gonzalez-García, C., Dalby, M.J. Salmeron-Sanchez, M., A tough act to follow: collagen hydrogel modifications to improve mechanical and growth factor loading capabilities, *Mat. Today Bio*., **2021**, *10*, 100098.
10. Antoine, E.E., Vlachos, P.P., Rylander, M.N., Review of collagen i hydrogels for bioengineered tissue microenvironments: Characterization of mechanics, structure, and transport, *Tissue Engineering - Part B: Reviews*. **2014**, *20*, 683–696.
11. Akther, F., Little, P., Li, Z., Nguyen, N.T., Ta, H.T., Hydrogels as artificial matrices for cell seeding in microfluidic devices, *RSC Adv.*, **2020**, *10*, 43682–43703.
12. Thiele, J., Ma, Y., Bruekers, S.M.C., Ma, S., Huck, W.T.S., 25th anniversary article: Designer hydrogels for cell cultures: A materials selection guide, *Adv. Mat*., **2013**, *26*, 125–148.
13. Yu, Z., Li, H., Xia, P., Kong, W., Chang, Y., Fu, C., Wang, K., Yang, X., Qi, Z., Application of fibrin-based hydrogels for nerve protection and regeneration after spinal cord injury, *Jour. of Bio. Eng*, **2020**, *14*, 22.
14. Lee, K.Y. and Mooney, D.J., Alginate: Properties and biomedical applications, *Prog, in Poly. Sci*., **2012**, *37*, 106–126.
15. Samani, S.M., Ahmadi, F., Oveisi, Z., Amoozgar, Z., Chitosan based hydrogels: characteristics and pharmaceutical applications, *PubMed*, **2015**, *10*, 1–16.
16. Andreazza, R., Morales, A., Pieniz, S., Labidi, J., Gelatin-Based Hydrogels: Potential Biomaterials for Remediation, *Polymers*, **2023**, *15*, 1026.

17. Xu, X., Jha, A.K., Harrington, D.A., Farach-Carson, M.C., Jia, X., Hyaluronic acid-based hydrogels: From a natural polysaccharide to complex networks, *Soft Matter*, **2012**, *8*, 3280–3294.

18. Burdick, J.A. and Prestwich G.D., Hyaluronic acid hydrogels for biomedical applications, *Advanced Materials*, **2011**, *23*, H41-H56 .

19. Larrañeta, E., Henry, M., Irwin, N.J., Trotter, J., Perminova A.A., Donnelly, R.F., Synthesis and characterization of hyaluronic acid hydrogels crosslinked using a solvent-free process for potential biomedical applications, *Carbohydr Polym.*, **2018**, *181*, 1194–1205.

20. Fan, D., Staufer, U., Accardo, A., Engineered 3d polymer and hydrogel microenvironments for cell culture applications, *Bioengineering*., **2019**, *6*, 113.

21. Zhu, J., Bioactive modification of poly(ethylene glycol) hydrogels for tissue engineering, *Biomaterials*, **2010**, *31*, 4639–4656.

22. Chen, Y., Li, J., Lu, J., Ding, M., Chen, Y., Synthesis and properties of Poly(vinyl alcohol) hydrogels with high strength and toughness, *Polym. Test.*, **2022**, *108*, 107516.

23. Wang, M., Bai, J., Shao, K., Tang, W., Zhao, X., Lin, D., Huang, S., Chen, C., Ding, Z., Ye, J., Poly(vinyl alcohol) Hydrogels: The Old and New Functional Materials, *Int. Jour. of Pol. Sci.*. **2021**, *2021*, 1–16.

24. Kulkarni, N., Rao, P., Jadhav, G.S., Kulkarni, B., Kanakavalli, N., Kirad, S., Salunke, S., Tanpure, V., Sahu, B., Emerging Role of Injectable Dipeptide Hydrogels in Biomedical Applications, *ACS Omega*, **2022**, *8*, 3551–3570.

25. Li, L., Xie, L., Zheng, P., Sun, R., Self-Assembly Dipeptide Hydrogel: The Structures and Properties. *Front. in Chem*., **2021**, *9*, 739791.

26. Colquhoun, C., Draper, E.R., Schweins, R., Marcello, M., Vadukul, D., Serpell, L.C., Adams D.J., Controlling the network type in self-assembled dipeptide hydrogels, *Soft Matter* **2017**, *13*, 1914–1919.

27. Bellotto, O., Kralj, S., Melchionna, M., Pengo, P., Kisovec, M., Podobnik, M., De Zorzi, R., Marchesan, S., Self-Assembly of Unprotected Dipeptides into Hydrogels: Water-Channels Make the Difference, *ChemBioChem*, **2022**, *23*, e202100518.

28. Palmese, L.L., Thapa, R.K., Sullivan, M.O., Kiick, K.L., Hybrid hydrogels for biomedical applications. *Current Opinion in Chem. Eng*., **2019**, *24*, 143–157.

29. Vasile, C., Pamfil, D., Stoleru, E., Baican, M., New developments in medical applications of hybrid hydrogels containing natural polymers, *Molecules*., **2020**, *25*, 1539.

30. Cai, M.H., Chen, X.Y., Fu, L.Q., Du, W.L., Yang, X., Mou, X.Z., Hu, P.Y., Design and Development of Hybrid Hydrogels for Biomedical Applications: Recent Trends in Anticancer Drug Delivery and Tissue Engineering, *Front. in Bioeng. and Biotech*., **2021**, *9*, 630943.

31. Zhan, X., *Cell Culture - Advanced Technology and Applications in Medical and Life Sciences*, InTechOpen, London, United Kingdom, 2022, pp. 2-6.

32. Segeritz, C.P., Vallier. L., Cell Culture: Growing Cells as Model Systems In Vitro in *Basic Science Methods for Clinical Researchers*, Academic Press, Cambridge, United Kingdom, 2017, pp. 151–172.

33. Duval, K., Grover, H., Han, L.H., Mou, Y., Pegoraro, A.F., Fredberg, J., Chen, Z., Modeling physiological events in 2D vs. 3D cell culture, *Physiology*, **2017**, *32*, 266–277.

34. Jensen, C. and Teng, Y., Is It Time to Start Transitioning From 2D to 3D Cell Culture?, *Front. in Mol. Biosci*., **2020,** *7*, 33.

35. Tibbitt, M.W. and Anseth, K.S., Hydrogels as extracellular matrix mimics for 3D cell culture, *Biotech. and Bioeng*., **2009**, *103*, 655–663.

36. Singh, N., Vayer, P., Tanwar, S., Poyet, J-L., Tsaioun, K., Villoutreix, B.O., Drug discovery and development: introduction to the general public and patient groups, *Frontiers in Drug Discovery*, **2023**, *3*, 1201419.

37. Harrison, I.P. and Spada, F., Hydrogels for atopic dermatitis and wound management: A superior drug delivery vehicle, *Pharmaceutics*., **2018**, *10*, 71.

38. Lee, S.H., Shim, K.Y., Kim, B., Sung, J.H., Hydrogel-based three-dimensional cell culture for organ-on-a-chip applications, *Biotech. Prog*., **2017**, *33*, 580–589.

39. Chaudhary, S. and Chakraborty E., Hydrogel based tissue engineering and its future applications in personalized disease modeling and regenerative therapy. *Beni-Suef Uni. Jour. of Basic and App. Sci*., **2022**, *11*, 3.

40. Grabska-Zielińska, S., Sionkowska, A., Carvalho, Â., Monteiro, F.J., Biomaterials with potential use in bone tissue regeneration-collagen/chitosan/silk fibroin scaffolds cross-linked by EDC/NHS, *Materials* **2021**, *14*, 1–21.

41. Tsou, Y.H., Khoneisser, J., Huang, P.C., Xu, X., Hydrogel as a bioactive material to regulate stem cell fate, *Bioactive Materials*., **2016**, *1*, 39–55.

42. Basu, P., Saha, N., Saha, T., Saha, P., Polymeric hydrogel based systems for vaccine delivery: A review, *Polymer*., **2021**, *230*, 124088.

43. Chalard, A., Vaysse, L., Joseph, P., Malaquin, L, Souleille, S., Lonetti, B., Sol, J.C., Loubinoux I., Fitremann, J., Simple Synthetic Molecular Hydrogels from Self-Assembling Alkylgalactonamides as Scaffold for 3D Neuronal Cell Growth, *ACS Appl. Mater. Interfaces,* **2018**, *10*, 17004–17017.

44. Kemper, B., Hristova, Y. R., Tacke, S., Stegemann, L., Van Bezouwen, L. S., Stuart, M. C. A., Klingauf, J., Strassert, C. A., & Besenius, P., Facile synthesis of a peptidic Au(I)-metalloamphiphile and its self-assembly into luminescent micelles in water, *Chem. Com.*, **2015**, *51*, 5253–5256.

LIST OF APPENDICES

APPENDIX 1

Qualitative Analysis Report

Data File	TJF5_02.d	**Sample Name**	TJF5
Sample Type	Sample	**Position**	
Instrument Name	Agilent 6560	**User Name**	
Acq Method	Dual AJS ESIQTOF AccMass.m	**Acquired Time**	11/30/2022 10:57:33 AM (UTC+02:00)
IRM Calibration Status	Success	**DA Method**	LC_caffeine_MGF.m
Comment	TJF5, stock 2 mM in DCM, sample 2ul/ml in MeOH, pos mode, flow 5, IMQTOF		
Method part to run:	Acquisition Only	**Sample Group**	
Info.		**Stream Name**	LC 1
Acquisition Time (Local)	11/30/2022 10:57:33 AM (UTC+02:00)	**Acquisition SW Version**	6200 series TOF/6500 series Q-TOF B.09.00 (B9044.1 SP1)
QTOF Driver Version	8.00.00	**QTOF Firmware Version**	24.723
Tune Mass Range Max.	3200		

Spectra

Fragmentor Voltage	Collision Energy	Ionization Mode
0	0	ESI

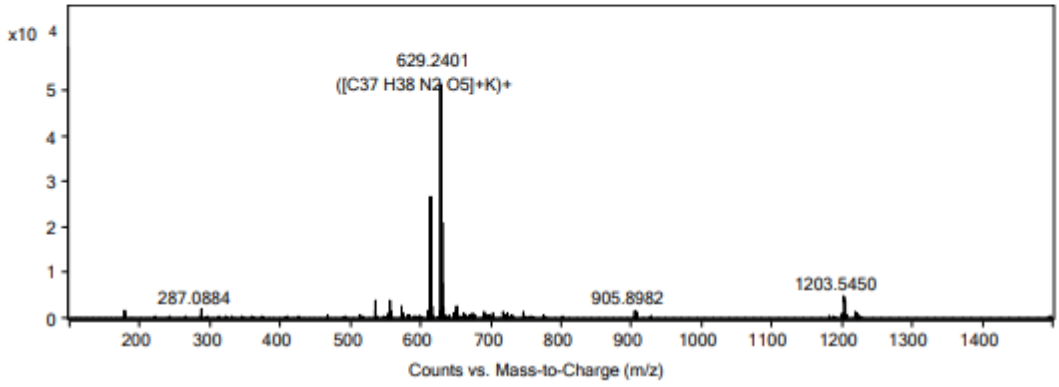

Peak List

m/z	z	Abund	Formula	Ion
613.2659	1	27362.81	C37 H38 N2 O5	(M+Na)+
629.2401	1	51386.16	C37 H38 N2 O5	(M+K)+
630.2433	1	20834.53	C37 H38 N2 O5	(M+K)+

Formula Calculator Element Limits

Element	Min	Max
C	37	37
H	38	38
O	5	5
N	2	2

Formula Calculator Results

Formula	Best	Mass	Tgt Mass	Diff (ppm)	Ion Species	Score
C37 H38 N2 O5	True	590.2764	590.2781	2.85	C37 H39 N2 O5	92.46
C37 H38 N2 O5	True	590.2767	590.2781	2.35	C37 H38 N2 Na O5	96.87
C37 H38 N2 O5	True	590.277	590.2781	1.87	C37 H38 K N2 O5	97.68

APPENDIX 2

Qualitative Analysis Report

Data File	TJF17_01.d	**Sample Name**	TJF17
Sample Type	Sample	**Position**	
Instrument Name	Agilent 6560	**User Name**	
Acq Method	Dual AJS ESIQTOF AccMass.m	**Acquired Time**	1/24/2023 12:57:37 PM (UTC+02:00)
IRM Calibration Status	Success	**DA Method**	AccMass_DA_new.m
Comment	TJF17 stock 1 mM in MeOH, sample 2 uM in MeOH, pos mode, flow 5,		
Method part to run:	Acquisition Only	**Sample Group**	
Info.		**Stream Name**	LC 1
Acquisition Time (Local)	1/24/2023 12:57:37 PM (UTC+02:00)	**Acquisition SW Version**	6200 series TOF/6500 series Q-TOF B.09.00 (B9044.1 SP1)
QTOF Driver Version	8.00.00	**QTOF Firmware Version**	24.723
Tune Mass Range Max.	3200		

Spectra

Fragmentor Voltage	Collision Energy	Ionization Mode
350	0	ESI

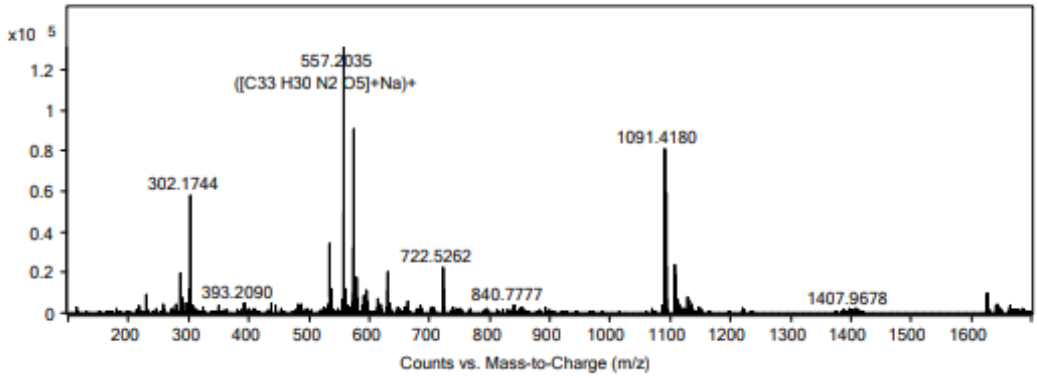

Peak List

m/z	z	Abund	Formula	Ion
557.2035	1	131299.43	C33 H30 N2 O5	(M+Na)+
573.1733	1	90686.22		
1091.418	1	81116.33		

Formula Calculator Element Limits

Element	Min	Max
C	33	33
H	30	30
O	5	5
N	2	2

Formula Calculator Results

Formula	Best	Mass	Tgt Mass	Diff (ppm)	Ion Species	Score
C33 H30 N2 O5	True	534.215	534.2155	0.85	C33 H31 N2 O5	99.24
C33 H30 N2 O5	True	534.214	534.2155	2.76	C33 H30 N2 Na O5	94.99

APPENDIX 3

Qualitative Analysis Report

Data File	OGX4_001.d	**Sample Name**	OGX-21
Sample Type	Sample	**Position**	
Instrument Name	Agilent 6560	**User Name**	
Acq Method	AJS_accurate mass QTOF.m	**Acquired Time**	6/8/2020 12:12:13 PM (UTC+03:00)
IRM Calibration Status	Success	**DA Method**	Accurate mass DA Uusi.m
Comment	OGX-21 in MeOH 1mg/ml DCM--> 5 ul/ml MeOH		
Method part to run:	Acquisition Only	**Sample Group**	
Info.		**Stream Name**	LC 1
Acquisition Time (Local)	6/8/2020 12:12:13 PM (UTC+03:00)	**Acquisition SW Version**	6200 series TOF/6500 series Q-TOF B.09.00 (B9044.1 SP1)
QTOF Driver Version	8.00.00	**QTOF Firmware Version**	24.723
Tune Mass Range Max.	1700		

Spectra

Fragmentor Voltage	Collision Energy	Ionization Mode
350	0	ESI

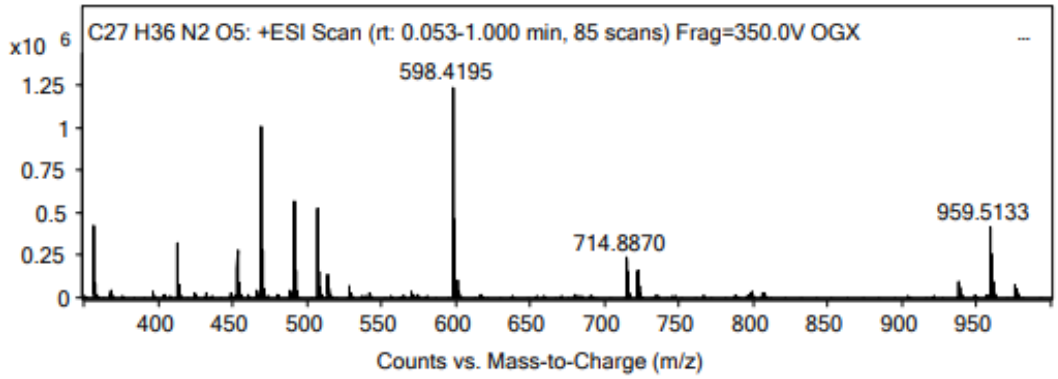

Peak List

m/z	z	Abund	Formula	Ion
130.1573		521689.91		
313.1525	1	597440.59	C15 H22 N O6	(M+H)+
357.1425	1	449518.38	C19 H20 N2 O5	(M+H)+
413.2058	1	321748.02	C23 H28 N2 O5	(M+H)+
469.2675	1	1059430.44	C27 H36 N2 O5	(M+H)+
491.2495	1	575523.38	C29 H34 N2 O5	(M+H)+
507.2236	1	529553.08	C32 H30 N2 O4	(M+H)+
598.4195	1	1301037.8		
599.4235	1	477798.81		
959.5133	1	428614.02		

Formula Calculator Element Limits

Element	Min	Max
C	10	40
H	10	40
O	0	6
N	0	2
P	0	0
F	0	0

APPENDIX 4

Sample Name	OGX-20	**Position**		**Instrument Name**	Agilent 6560
User Name		**Inj Vol**	0	**InjPosition**	
Sample Type	Sample	**IRM Calibration Status**	Success	**Data Filename**	OGX20_002.d
ACQ Method	AJS_accurate mass QTOF.m	**Comment**	OGX-20 xerogel in MeOH 1mg/ml DCM--> 5 ul/ml MeOH	**Acquired Time**	8.6.2020 12:38:41 (UTC+03:00)

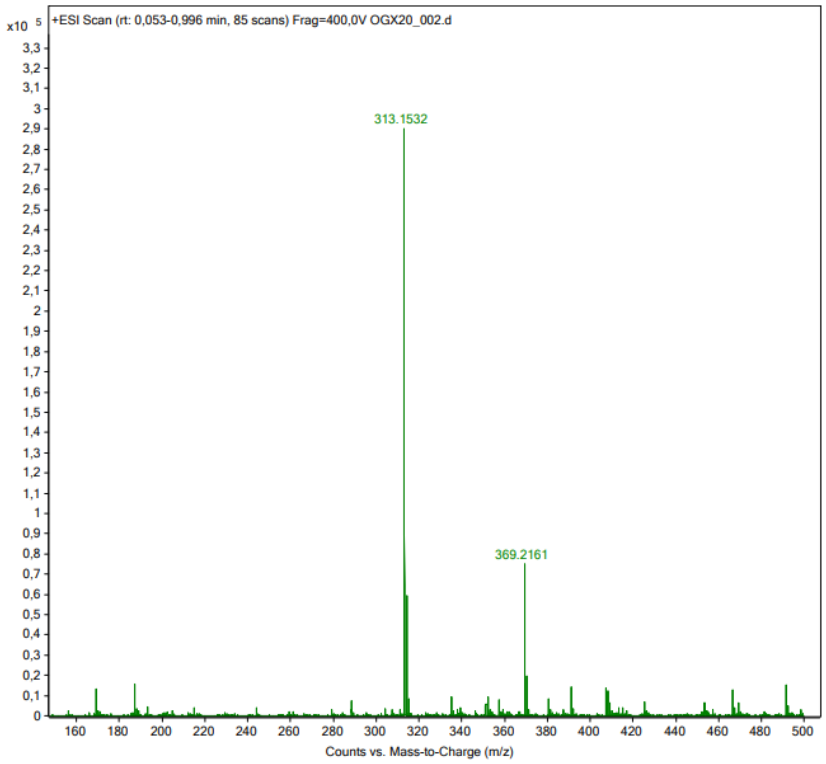

APPENDIX 5

Qualitative Analysis Report

Data File	TJF7B_01.d	**Sample Name**	TJF7B
Sample Type	Sample	**Position**	
Instrument Name	Agilent 6560	**User Name**	
Acq Method	Dual AJS ESIQTOF AccMass.m	**Acquired Time**	12/9/2022 1:35:47 PM (UTC+02:00)
IRM Calibration Status	Success	**DA Method**	LC_caffeine_MGF.m
Comment	TJF7B,stock 1mM in DCM, sample SuM in MeOH, pos mode, flow 5, QTOF only		
Method part to run:	Acquisition Only	**Sample Group**	
Info.		**Stream Name**	LC 1
Acquisition Time (Local)	12/9/2022 1:35:47 PM (UTC+02:00)	**Acquisition SW Version**	6200 series TOF/6500 series Q-TOF B.09.00 (B9044.1 SP1)
QTOF Driver Version	8.00.00	**QTOF Firmware Version**	24.723
Tune Mass Range Max.	3200		

Spectra

Fragmentor Voltage	Collision Energy	Ionization Mode
350	0	ESI

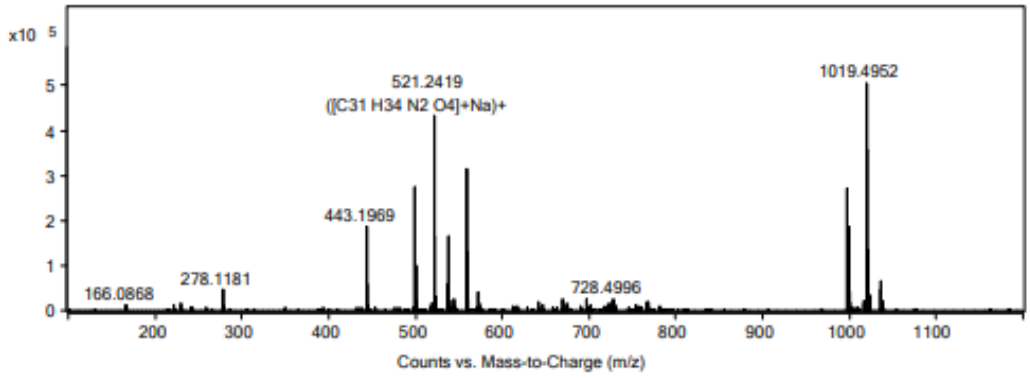

Peak List

m/z	z	Abund	Formula	Ion
521.2419	1	435239.47	C31 H34 N2 O4	(M+Na)+
1019.4952	1	506058.37		
1020.498	1	370708.87		

Formula Calculator Element Limits

Element	Min	Max
C	31	31
H	34	34
O	4	4
N	0	2

Formula Calculator Results

Formula	Best	Mass	Tgt Mass	Diff (ppm)	Ion Species	Score
C31 H34 N2 O4	True	498.2522	498.2519	-0.6	C31 H35 N2 O4	98.92
C31 H34 N2 O4	True	498.2524	498.2519	-1.19	C31 H34 N2 Na O4	97.36